Applied Mathematical Modelling 119 (2023) 99–118

Contents lists available at ScienceDirect

Applied Mathematical Modelling

journal homepage: www.elsevier.com/locate/apm

A fractional order age-specific smoke epidemic model

Emmanuel Addai[a,b], Lingling Zhang[b,*], Joshua K. K. Asamoah[c,*], John Fiifi Essel[d]

[a] College of Biomedical Engineering, Taiyuan University of Technology, Shanxi Taiyuan 030024, China
[b] Department of Mathematics, Taiyuan University of Technology, Shanxi Taiyuan 030024, China
[c] Department of Mathematics, Kwame Nkrumah University of Science and Technology, Kumasi, Ghana
[d] Department of Mathematics and Statistics, Portland State University, Oregon, United State of America

ARTICLE INFO

Article history:
Received 15 January 2022
Revised 4 February 2023
Accepted 10 February 2023
Available online 23 February 2023

Keywords:
Smoke epidemiology
Atangana-Baleanu-Caputo derivative
Hyers-Ulam stability
Numerical simulation

ABSTRACT

This paper presents a nonlinear fractional mathematical model for the smoke epidemic that includes two age groups. To solve the smoke epidemic, the Atangana-Baleanu-Caputo fractional derivative is used. The Banach and Krasnoselskii type fixed point theorem is used to determine existence and uniqueness. We explored model stability using the Hyers-Ulam form of stability. Using Lagrange interpolation, the behaviour of the smoke epidemic of the 2-age group model is generated. The numerical simulation shows that the model has potential for both groups, and that age-specific interventions can be used to reduce smoking rates in the general population.

1. Introduction

Numerous infectious diseases can be studied using mathematical models incorporating a set of nonlinear differential equations. Mathematical models addressing transmission dynamics, control, and other topics have been produced over the past few decades. Researchers have been paying close attention to the fractional calculus since 2000, thanks to the introduction of numerous types of fractional derivatives [1–3]. The advantage of fractional derivatives is that they can better depict the dynamics and other properties of hereditary materials. As a result, different biological models have been studied using Caputo and Riemann-Liouville fractional derivatives which involve singular kernels [4]. The singular kernels lead to several challenges during conventional procedures. To alleviate the drawbacks of such kernels, derivatives with nonsingular kernel were devolved by Caputo and Fabrizio (CF) [5]; see [6,7] for more details about CF-fractional derivatives. One of the most well-known fractional derivatives that recently has received interest from scientists is the Atangana-Baleanu-Caputo (ABC) fractional derivative. In the work of Atangana and Baleanu, they came up with a new type of nonsingular derivative using the Mittag-Leffler function [8,9]. Many researchers have used ABC derivative-type for infectious diseases models. All the findings have shown to be significant and useful in comprehending the dynamics of real-world occurrences. Not long ago, in [10], the authors analyzed the transmission dynamics of the COVID-19 mathematical model under the ABC fractional order derivative where existence-uniqueness, stability and simulation solutions were established; see [11–16] for more details about ABC fractional derivatives.

Tobacco is the main carcinogen that has been detected all over the world. Smokers are 10 to 30 times more likely than non-smokers to acquire lung cancer [17]. The smoking-related disease has become a major public health concern. Smoking

* Corresponding authors.
E-mail addresses: papayawewit@gmail.com (E. Addai), tyutzll@126.com (L. Zhang), jkkasamoah@knust.edu.gh (J.K. K. Asamoah), esselfiifijohn24@gmail.com (J.F. Essel).

https://doi.org/10.1016/j.apm.2023.02.019
0307-904X/

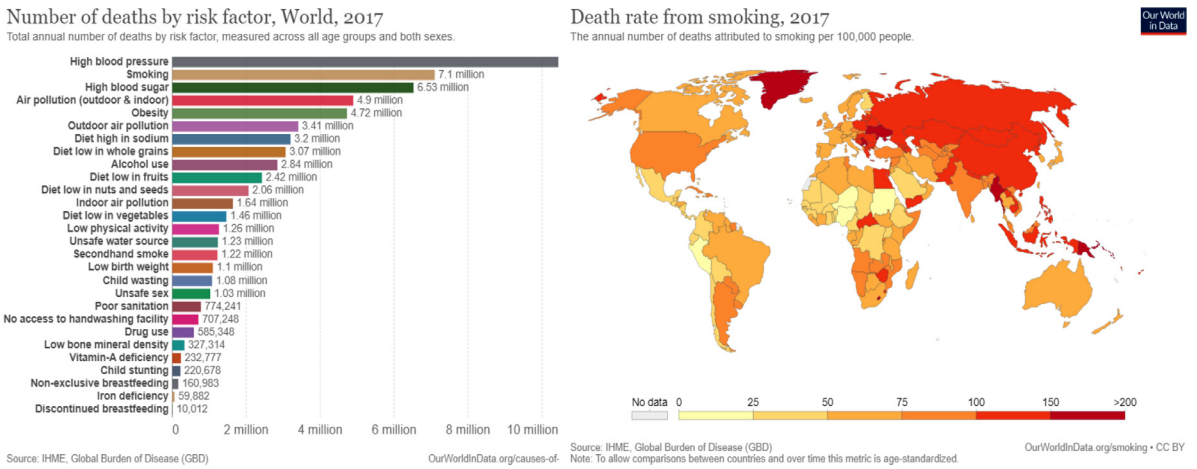

(a) The risk factor of smoke epidemic disease compare to other disease, 2017 [26].

(b) Global death of smoke epidemic disease, 2017 [26].

Fig. 1. The risk factor and death rate of smoke epidemic disease, 2017 [26].

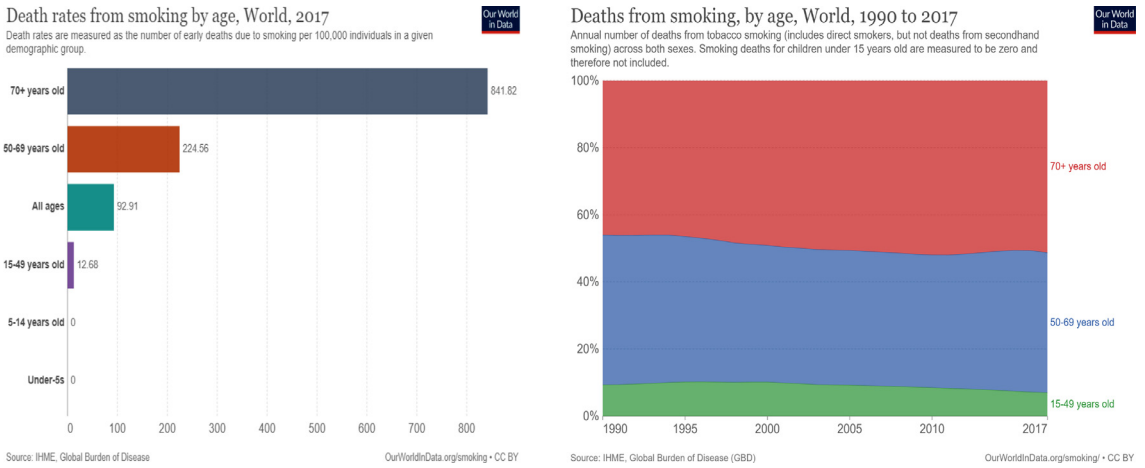

Fig. 2. Death rate from smoking by ages up to 2017, image adopted from [26].

behavior frequently has a variety of harmful outcomes [17]. Smoking causes unfavorable effects on the heart, such as an increase in heart rate and blood pressure [18,19]. Smoking causes damage to nearly every area of the human body and contributes to a variety of diseases such as lung cancer, respiratory disease, heart disease, alimentary canal effect with consequent increased mortality [20–22]. Because of the rising number of smokers, tobacco use is now considered an illness that must be treated. Fig. 1 and Fig. 2 give a pictorial nature of the smoke epidemic and its deaths.

In recent years, a slew of mathematical models of smoking has been developed by [23–25]. The work of these authors addresses a scheme with a total unchanging community which is split up into five classes: Potential smokers (P); Occasional smokers (Q); Smokers (S); Smokers who temporarily quit smoking (R); Smokers who permanently quit smoking (U). The model which contains the ordinary derivative as provided by [23–25] is as follows;

$$\begin{cases} \frac{dP}{dt} = \Lambda - \beta SP - \mu P, \\ \frac{dQ}{dt} = \beta SP - \lambda Q - \mu Q, \\ \frac{dS}{dt} = \lambda Q + \nu QS - (\mu + \eta)S, \\ \frac{dR}{dt} = \eta(1-\delta)S - \nu QS - \mu R, \\ \frac{dU}{dt} = \eta\delta S - \mu U. \end{cases}$$

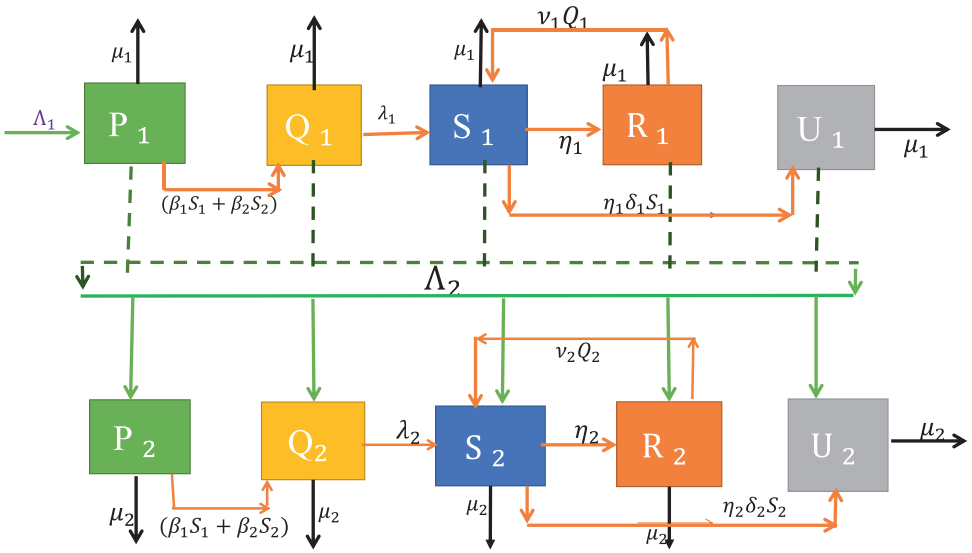

Fig. 3. Transfer diagram for the dynamism transmission of 2-age group smoke model.

Table 1
Interpretation of state variables in the model.

Parameter	Interpretation
N_1, N_2	Total population size for Group 1 and Group 2
P_1, P_2	Potential smokers for Group 1 and Group 2
Q_1, Q_2	Occasional smokers for Group 1 and Group 2
S_1, S_2	Smokers for Group 1 and Group 2
R_1, R_2	Smokers who temporarily quit smoking for Group 1 and Group 2
U_1, U_2	Smokers who permanently quit smoking for Group 1 and Group 2

Table 2
Interpretation of parameters in the model .

Parameter	value	Interpretation
$\Lambda_1^{\mu_*}$	$1-10$ (day^{-1})	recruitment rate of Group 1
Λ_2	0.001 (day^{-1})	recruitment rate of Group 2 (G2)
$\beta_{\mu_* 1}$	0.0014 (day^{-1})	effective contact rate between S_1 and P_1
$\beta_2^{\mu_*}$	0.0016667 (day^{-1})	effective contact rate between S_2 and P_2
$\mu_1^{\mu_*}, \mu_2^{\mu_*}$	0.00002, 0.0040 (day^{-1})	natural death rate for Group 1 (G1) and G2
λ_1, λ_2	0.00068, 0.00021 (day^{-1})	the rate at which occasional smokers become regular smokers for G1 and G2,
$\eta_1^{\mu_*}, \eta_2^{\mu_*}$	0.00245, 0.00078 (day^{-1})	the rate of quitting smoking for both Group 1 and Group 2
$\nu_1^{\mu_*}, \nu_2^{\mu_*}$	0.0019, 0.0087 (day^{-1})	the contact rate between smokers and temporary quitters
$\delta_1^{\mu_*}, \delta_2^{\mu_*}$	0.001, 0.001 (day^{-1})	the remaining fraction of smokers who permanently quit smoking

The basic reproduction number($\mathcal{R}_0$) is defined as follows;

$$\mathcal{R}_0 = \frac{\lambda\beta}{(c+\mu+\delta)(c+\lambda+\mu)}.$$

More detailed descriptions of variables and parameters are listed in Table 1 and Table 2.

Motivated by the aforementioned literature and [29], to the best of our knowledge, there is no mathematical model for the smoking epidemic that considers two age-group specific. Hence, this paper contributes to the existing knowledge on the spread of tobacco-related diseases and the dynamic influence of the diseases in the 2-age groups. The smoking epidemic model not only extends to two age-group specific but also it gives a mathematical interpretation of the use of real data set published in some literature. The rest of this paper is structured as follows; Some key ideas, fundamental definitions, and preliminary findings are all briefly introduced in Section 2. In Section 3 we formulate age-group specific model and briefly describe all the parameters. The mathematical analysis of the existence-uniqueness of age-group-specific models is covered in Section 4. In Section 5, the stability findings of the age-group-specific model are presented and analysed. In Section 6 and Section 7, discusses the numerical outcomes and graphic display. In Section 8, concludes the paper.

2. Preliminaries

In this section, we recall some critical concepts, lemmas, and definitions to study the system (2).

Definition 2.1. [10]. The ABC-fractional differential operator on $\Upsilon \in H^1(a,b)$, for $\mu_* \in [0,1)$ is

$$^{ABC}D_t^{\mu_*}\Upsilon(t) = \frac{\aleph(\mu_*)}{1-\mu_*}\int_0^t \Upsilon'(s)E_{\mu_*}\left[\frac{-\mu_*(t-s)^{\mu_*}}{1-\mu_*}\right]ds,$$

which approaches the ordinary derivative as $\mu_* \to 1$, also $\aleph(\mu_*)$ satisfies the property $\aleph(1) = \aleph(0) = 1$. And E_{μ_*} is a Mittag-Leffler function, which is defined as follows

$$E_{\mu_*}(t) = \sum_{k=0}^{\infty}\frac{t^k}{\Gamma(\mu_* k+1)}.$$

Definition 2.2. [13],[14]. For $\Upsilon \in H^1(a,b)$, for $\mu_* \in (0,1)$, then the integral of ABC is given by

$$^{ABC}I_t^{\mu_*}\Upsilon(t) = \frac{1-\mu_*}{\aleph(\mu_*)}\Upsilon(t) + \frac{\mu_*}{\aleph(\mu_*)\Gamma(\mu_*)}\int_0^t \Upsilon(s)(t-s)^{\mu_*-1}ds,$$

assuming that the integral on the right converges.

Lemma 2.3. *[10]. The definitions of ABC-fractional derivative of the function Υ and the corresponding fractional integral, satisfy the Newton-Leibniz formula*

$$^{ABC}I_t^{\mu_*}(^{ABC}D_t^{\mu_*}\Upsilon(t)) = \Upsilon(t) - \Upsilon(\mu_*).$$

Lemma 2.4. [30,31]. *Consider a function $F(t) \in C[0,\eta]$ then the solution of fractional differential equation*

$$\begin{cases} ^{ABC}D_{0+}^{\mu_*}\Upsilon(t) = F(t), t \in [0,\eta], \\ \Upsilon(0) = F_0, \end{cases}$$

is given by

$$\Upsilon(t) = F_0 + \frac{1-\mu_*}{\aleph(\mu_*)}F(t) + \frac{\mu_*}{\aleph(\mu_*)\Gamma(\mu_*)}\int_0^t F(s)(t-s)^{\mu_*-1}ds.$$

Now, we let $\boldsymbol{M}^* = C^*([0,\eta])$ be a Banach space with the following norm

$$||\Upsilon|| = \max_{t\in[0,\eta]}\{|\Upsilon|\},\ \forall \Upsilon \in \boldsymbol{M}^*.$$

Lemma 2.5. *[15]. Suppose $\boldsymbol{B}^* \subset \boldsymbol{M}^*$, be a closed convex non-empty subset of $\boldsymbol{M}^*$ and there exist two operators T_1 and T_2 then it is Krassnoselskii's fixed point theorem and it follows that;*

(i) $T_1u + T_1u \in \boldsymbol{M}^*,\ \forall u \in \boldsymbol{M}^*$;

(ii) T_1 is a contraction operator and T_2 continuous and compact. Then $\exists$ at least one solution $u \in \boldsymbol{M}^*$ such that

$$T_1u + T_2u = u.$$

3. Model formulation

We consider an extension of the smoke epidemic model considered by [23–25] to a 2-age group model (1) by incorporating age-specific parameters. From here, we represent the 1-Group by people below 70 years old (<70 years), and the 2-group includes the people from 70 years (≥ 70 years). Each population ($PQSRU$) consist of $P_1+Q_1+S_1+R_1+U_1$ for 1-Group and $P_2+Q_2+S_2+R_2+U_2$ for 2-Group. $N(t) = N_1+N_2$ and $N_i = P_i+Q_i+S_i+R_i+U_i$ where $i = 1,2$. For each i-age group, β_i is the effective contact rate between P_i and S_i, and λ_i is the rate at which occasional smokers become regular smokers. Further, μ_i natural death rate, while η_i is the rate of quitting smoking. Similarly, $(1-\delta_i)$ is the fraction of smokers who temporary quit smoking (at the rate η_i), whilst δ_1 is the remaining fraction of smokers who permanently quit. Also ν_i is the contact rate between smokers and temporary quitters who revert back to smoking. In the same way, Λ_1 is the rate of supply to susceptible age at adolescence P_1, and we assume that 1-Group (the young age group) move to 2-Group (the old age group) by the proportion of 2-Group is Λ_2. Hence, the 2-age group transmission model is described by the following

system of differential equations.

$$\begin{cases} \frac{dP_1(t)}{dt} = \Lambda_1 - (\beta_1 S_1 + \beta_2 S_2)P_1 - \mu_1 P_1 - \Lambda_2 P_1, \\ \frac{dQ_1(t)}{dt} = (\beta_1 S_1 + \beta_2 S_2)P_1 - \lambda_1 Q_1 - \mu_1 Q_1 - \Lambda_2 Q_1, \\ \frac{dS_1(t)}{dt} = \lambda_1 Q_1 + \nu_1 Q_1 S_1 - (\mu_1 + \eta_1)S_1 - \Lambda_2 S_1, \\ \frac{dR_1(t)}{dt} = \eta_1(1-\delta_1)S_1 - \nu_1 Q_1 S_1 - \mu_1 R_1 - \Lambda_2 R_1, \\ \frac{dU_1(t)}{dt} = \eta_1 \delta_1 S_1 - \mu_1 U_1 - \Lambda_2 U_1, \\ \frac{dP_2(t)}{dt} = \Lambda_2 P_1 - (\beta_1 S_1 + \beta_2 S_2)P_2 - \mu_2 P_2, \\ \frac{dQ_2(t)}{dt} = \Lambda_2 Q_1 + (\beta_1 S_1 + \beta_2 S_2)P_2 - \lambda_2 Q_2 - \mu_2 Q_2, \\ \frac{dS_2(t)}{dt} = \Lambda_2 S_1 + \lambda_2 Q_2 + \nu_2 Q_2 S_2 - (\mu_2 + \eta_2)S_2, \\ \frac{dR_2(t)}{dt} = \Lambda_2 R_1 + \eta_2(1-\delta_2)S_2 - \nu_2 Q_2 S_2 - \mu_2 R_2, \\ \frac{dU_2(t)}{dt} = \Lambda_2 U_1 + \eta_2 \delta_2 S_2 - \mu_2 U_2. \end{cases} \tag{1}$$

According to the explanation of time-dependent kernel defined by the Mittag-Leffler kernel function, presented in [32] and [34], our considered 2-age group smoke transmission model under ABC fractional derivative is defined as follows;

$$\begin{cases} {}^{ABC}_{0}D_t^{\mu_*} P_1(t) = \Lambda_1^{\mu_*} - (\beta_1^{\mu_*} S_1 + \beta_2^{\mu_*} S_2)P_1 - \mu_1^{\mu_*} P_1 - \Lambda_2^{\mu_*} P_1, \\ {}^{ABC}_{0}D_t^{\mu_*} Q_1(t) = (\beta_1^{\mu_*} S_1 + \beta_2^{\mu_*} S_2)P_1 - \lambda_1^{\mu_*} Q_1 - \mu_1^{\mu_*} Q_1 - \Lambda_2^{\mu_*} Q_1, \\ {}^{ABC}_{0}D_t^{\mu_*} S_1(t) = \lambda_1^{\mu_*} Q_1 + \nu_1^{\mu_*} Q_1 S_1 - (\mu_1^{\mu_*} + \eta_1^{\mu_*})S_1 - \Lambda_2^{\mu_*} S_1, \\ {}^{ABC}_{0}D_t^{\mu_*} R_1(t) = \eta_1^{\mu_*}(1-\delta_1^{\mu_*})S_1 - \nu_1^{\mu_*} Q_1 S_1 - \mu_1^{\mu_*} R_1 - \Lambda_2^{\mu_*} R_1, \\ {}^{ABC}_{0}D_t^{\mu_*} U_1(t) = \eta_1^{\mu_*} \delta_1^{\mu_*} S_1 - \mu_1^{\mu_*} U_1 - \Lambda_2^{\mu_*} U_1, \\ {}^{ABC}_{0}D_t^{\mu_*} P_2(t) = \Lambda_2^{\mu_*} P_1 - (\beta_1^{\mu_*} S_1 + \beta_2^{\mu_*} S_2)P_2 - \mu_2^{\mu_*} P_2, \\ {}^{ABC}_{0}D_t^{\mu_*} Q_2(t) = \Lambda_2^{\mu_*} Q_1 + (\beta_1^{\mu_*} S_1 + \beta_2^{\mu_*} S_2)P_2 - \lambda_2^{\mu_*} Q_2 - \mu_2^{\mu_*} Q_2, \\ {}^{ABC}_{0}D_t^{\mu_*} S_2(t) = \Lambda_2^{\mu_*} S_1 + \lambda_2^{\mu_*} Q_2 + \nu_2^{\mu_*} Q_2 S_2 - (\mu_2^{\mu_*} + \eta_2^{\mu_*})S_2, \\ {}^{ABC}_{0}D_t^{\mu_*} R_2(t) = \Lambda_2^{\mu_*} R_1 + \eta_2^{\mu_*}(1-\delta_2^{\mu_*})S_2 - \nu_2^{\mu_*} Q_2 S_2 - \mu_2^{\mu_*} R_2, \\ {}^{ABC}_{0}D_t^{\mu_*} U_2(t) = \Lambda_2^{\mu_*} U_1 + \eta_2^{\mu_*} \delta_2^{\mu_*} S_2 - \mu_2^{\mu_*} U_2, \end{cases} \tag{2}$$

with initial condition

$$P_1(0) = P_{1_{(0)}},\ Q_1(0) = Q_{1_{(0)}},\ S_1(0) = S_{1_{(0)}},\ R_1(0) = R_{1_{(0)}},\ U_1(0) = U_{1_{(0)}},$$

$$P_2(0) = P_{2_{(0)}},\ Q_2(0) = Q_{2_{(0)}},\ S_2(0) = S_{2_{(0)}},\ R_2(0) = R_{2_{(0)}},\ U_2(0) = U_{2_{(0)}}.$$

4. Existence and uniqueness results for the 2-age group smoke transmission model

We reformulate the right side of the model (2) as follows;

$$\begin{cases} \Upsilon_1(t, P_i + Q_i + S_i + R_i + U_i) = \Lambda_1^{\mu_*} - (\beta_1^{\mu_*} S_1 + \beta_2^{\mu_*} S_2)P_1 - \mu_1^{\mu_*} P_1 - \Lambda_2^{\mu_*} P_1, \\ \Upsilon_2(t, P_i + Q_i + S_i + R_i + U_i) = (\beta_1^{\mu_*} S_1 + \beta_2^{\mu_*} S_2)P_1 - \lambda_1^{\mu_*} Q_1 - \mu_1^{\mu_*} Q_1 - \Lambda_2^{\mu_*} Q_1, \\ \Upsilon_3(t, P_i + Q_i + S_i + R_i + U_i) = \lambda_1^{\mu_*} Q_1 + \nu_1^{\mu_*} Q_1 S_1 - (\mu_1^{\mu_*} + \eta_1^{\mu_*})S_1 - \Lambda_2^{\mu_*} S_1, \\ \Upsilon_4(t, P_i + Q_i + S_i + R_i + U_i) = \eta_1^{\mu_*}(1-\delta_1^{\mu_*})S_1 - \nu_1^{\mu_*} Q_1 S_1 - \mu_1^{\mu_*} R_1 - \Lambda_2^{\mu_*} R_1, \\ \Upsilon_5(t, P_i + Q_i + S_i + R_i + U_i) = \eta_1^{\mu_*} \delta_1^{\mu_*} S_1 - \mu_1^{\mu_*} U_1 - \Lambda_2^{\mu_*} U_1, \\ \Upsilon_6(t, P_i + Q_i + S_i + R_i + U_i) = \Lambda_2^{\mu_*} P_1 - (\beta_1^{\mu_*} S_1 + \beta_2^{\mu_*} S_2)P_2 - \mu_2^{\mu_*} P_2, \\ \Upsilon_7(t, P_i + Q_i + S_i + R_i + U_i) = \Lambda_2^{\mu_*} Q_1 + (\beta_1^{\mu_*} S_1 + \beta_2^{\mu_*} S_2)P_2 - \lambda_2^{\mu_*} Q_2 - \mu_2^{\mu_*} Q_2, \\ \Upsilon_8(t, P_i + Q_i + S_i + R_i + U_i) = \Lambda_2^{\mu_*} S_1 + \lambda_2^{\mu_*} Q_2 + \nu_2^{\mu_*} Q_2 S_2 - (\mu_2^{\mu_*} + \eta_2^{\mu_*})S_2, \\ \Upsilon_9(t, P_i + Q_i + S_i + R_i + U_i) = \Lambda_2^{\mu_*} R_1 + \eta_2^{\mu_*}(1-\delta_2^{\mu_*})S_2 - \nu_2^{\mu_*} Q_2 S_2 - \mu_2^{\mu_*} R_2, \\ \Upsilon_{10}(t, P_i + Q_i + S_i + R_i + U_i) = \Lambda_2^{\mu_*} U_1 + \eta_2^{\mu_*} \delta_2^{\mu_*} S_2 - \mu_2^{\mu_*} U_2. \end{cases} \tag{3}$$

Where $i = 1, 2$ and from (3), the generated model (2) can be expressed as

$$\begin{cases} {}^{ABC}_{0}D_t^{\mu_*} \Upsilon(t) = \Psi(t, \Upsilon(t)),\ t \in [0, \eta],\ 0 < \mu_* \leq 1, \\ \Upsilon(0) = \Upsilon_0, \end{cases} \tag{4}$$

where

$$\Upsilon(\sigma)=\begin{cases}P_i(t),\\ Q_i(t),\\ S_i(t),\\ R_i(t),\\ U_i(t),\end{cases}\quad \Upsilon_0=\begin{cases}P_i(0),\\ Q_i(0),\\ S_i(0),\\ R_i(0),\\ U_i(0),\end{cases} \tag{5}$$

for all $i=1,2$.

$$\Psi(t,\Upsilon(t))=\begin{cases}\Upsilon_1(t,P_i+Q_i+S_i+R_i+U_i),\\ \Upsilon_2(t,P_i+Q_i+S_i+R_i+U_i),\\ \Upsilon_3(t,P_i+Q_i+S_i+R_i+U_i),\\ \Upsilon_4(t,P_i+Q_i+S_i+R_i+U_i),\\ \Upsilon_5(t,P_i+Q_i+S_i+R_i+U_i).\end{cases} \tag{6}$$

Using the ideas in Lemma 2.4, system (4) yields,

$$\begin{cases}\Upsilon(t)=\Upsilon_0(t)+\frac{1-\mu_*}{\aleph(\mu_*)}\Psi(t,\Upsilon(t))+\frac{\mu_*}{\aleph(\mu_*)\Gamma(\mu_*)}\\ \qquad\times\int_0^t\Psi(s,\Upsilon(s))(t-s)^{\mu_*-1}ds.\end{cases} \tag{7}$$

We consider the Banach space $\boldsymbol{B}_*=C([0,\eta])$, and assume that assumptions below hold

(F_1) There $\exists$ a positive constant Y_*, Z_*, and $k_*\in[0,1)$ such that

$$\Psi(t,\Upsilon(t))\le Y_*|\Upsilon|^{k_*}+Z_*.$$

(F_2) There $\exists$ a positive constant $\mathbf{L}_\rho>0\ \forall\ \Upsilon,\tilde{\Upsilon}\in\boldsymbol{B}_*$ then

$$|\Psi(t,\Upsilon(t))-\Psi(t,\tilde{\Upsilon}(t))|\le\mathbf{L}_\rho[|\Upsilon-\tilde{\Upsilon}|].$$

Suppose that operator $\mathbf{A}_p:\boldsymbol{B}_*\to\boldsymbol{B}_*$ such that

$$\mathbf{A}_p\Upsilon(t)=\Omega_1^*\Upsilon(t)+\Omega_2^*\Upsilon(t),$$

basically, we can see that

$$\begin{cases}\Omega_1^*\Upsilon(t)=\Upsilon_0+\frac{1-\mu_*}{\aleph(\mu_*)}\Psi(t,\Upsilon(t)),\\ \Omega_2^*\Upsilon(t)=\frac{\mu_*}{\aleph(\mu_*)\Gamma(\mu_*)}\int_0^t\Psi(s,\Upsilon(s))(t-s)^{\mu_*-1}ds.\end{cases} \tag{8}$$

From this knowledge (7) can be written as

$$\begin{cases}\mathbf{A}_p\Upsilon(t)=\Upsilon_0(t)+\frac{1-\mu_*}{\aleph(\mu_*)}\Psi(t,\Upsilon(t))+\frac{\mu_*}{\aleph(\mu_*)\Gamma(\mu_*)}\\ \qquad\times\int_0^t\Psi(s,\Upsilon(s))(t-s)^{\mu_*-1}ds.\end{cases} \tag{9}$$

Theorem 4.1. *Suppose that (F_1) and (F_2) hold, such that, $\frac{(1-\mu_*)}{\aleph(\mu_*)}\mathbf{L}_\rho<1$, then the 2-age group smoke transmission model has at least one solution.*

Proof. We break the proof into two steps for ease of understanding.

Step 1. We prove that operator Ω_1^* is a contraction. If so, let $\tilde{\Upsilon}\in\Pi$, such that $\Pi=\{\Upsilon\in\mathbf{B}_*:\ ||\Upsilon||\le\phi,\ \phi>0\}$ is a close convex set, thus

$$\begin{aligned}|\Omega_1^*\Upsilon(t)-\Omega_2^*\Upsilon(t)|&=\frac{(1-\mu_*)}{\aleph(\mu_*)}\max_{\mu_*\in[0,\eta]}|\Psi(t,\Upsilon(t))-\Psi(t,\tilde{\Upsilon}(t))|,\\ &\le\frac{(1-\mu_*)}{\aleph(\mu_*)}\mathbf{L}_\rho||\Upsilon-\tilde{\Upsilon}||.\end{aligned} \tag{10}$$

Thus,

$$||\Omega_1^*\Upsilon(t)-\Omega_2^*\Upsilon(t)||\le\frac{(1-\mu_*)}{\aleph(\mu_*)}\mathbf{L}_\rho||\Upsilon-\tilde{\Upsilon}||.$$

Hence Ω_1^* is contraction since $\frac{(1-\mu_*)}{\aleph(\mu_*)}\mathbf{L}_\rho<1$.

Step 2. We prove that Ω_2^* is compact and also continuous, $\forall\ \Upsilon\in\Pi$, then Ω_2^* will be continuous as Υ is continuous, thus

$$||\Omega_2^*(\Upsilon)||=\max_{\mu_*\in[0,\eta]}|\frac{\mu_*}{\aleph(\mu_*)\Gamma(\mu_*)}\int_0^\sigma\Psi(s,\Upsilon(s))(t-s)^{\mu_*-1}ds|,$$

$$\leq \frac{\mu_*}{\aleph(\mu_*)\Gamma(\mu_*)}\int_0^{\eta}|(\eta-s)^{\mu_*-1}|\ |\Psi(s,\Upsilon(s))|ds.$$
$$\leq \frac{\eta^{\mu_*}}{\aleph(\mu_*)\Gamma(\mu_*)}[Y_*|\Upsilon|^{k_*}+Z_*]. \tag{11}$$

Hence Ω_2^* is boundedness. Now we prove equicontinuous, let $t_1, t_2 \in [0,\eta]$, such that

$$|(\Omega_2^*\Upsilon)(t_1)-(\Omega_2^*\Upsilon)(t_2)| = |\frac{\mu_*}{\aleph(\mu_*)\Gamma(\mu_*)}\ |\int_0^{t_1}\Psi(s,\Upsilon(s))(t_1-s)^{\mu_*-1}ds$$
$$-\int_0^{t_2}\Psi(s,\Upsilon(s))(t_2-s)^{\mu_*-1}|ds$$
$$\leq \frac{[Y_*|\Upsilon|^{k_*}+Z_*]}{\aleph(\mu_*)\Gamma(\mu_*)}[t_1^{\mu_*}-t_2^{\mu_*}]. \tag{12}$$

As $\sigma_1 \to \sigma_2$, then $|(\Omega_2^*\Upsilon)(t_1)-(\Omega_2^*\Upsilon)(t_2)| \to 0$ which makes the operator Ω_2^* equicontinuous and compact by well-known Arzela-Ascoli theorem. Hence, by Lemma 2.5 the existence for the 2-age group smoke transmission model has at least one solution. □

Theorem 4.2. *The operator* $\mathbf{A}_p$ *has a unique fixed point, if there* $\exists$ *a positive constant* $\Lambda > 0$ *such that*

$$\Lambda = [\tfrac{(1-\mu_*)}{\aleph(\mu_*)}\mathbf{L}_\rho + \tfrac{\eta^{\mu_*}}{\aleph(\mu_*)\Gamma(\mu_*)}\mathbf{L}_\rho] < 1. \tag{13}$$

Proof. Let $\Upsilon, \tilde{\Upsilon} \in \boldsymbol{B}_*$, then we have

$$||\mathbf{A}_p\Upsilon-\mathbf{A}_p\tilde{\Upsilon}|| \leq ||\Omega_1^*\Upsilon-\Omega_1^*\tilde{\Upsilon}||+||\Omega_2^*\Upsilon-\Omega_2^*\tilde{\Upsilon}||,$$
$$\leq \frac{(1-\mu_*)}{\aleph(\mu_*)}|\max_{\mu_*\in[0,\eta]}|\Psi(t,\Upsilon(t))-\Psi(t,\tilde{\Upsilon}(t))|$$
$$+\frac{\mu_*}{\aleph(\mu_*)\Gamma(\mu_*)}\max_{\mu_*\in[0,\eta]}|\int_0^t\Psi(s,\Upsilon(s))(t-s)^{\mu_*-1}ds$$
$$-\int_0^t\Psi(s,\tilde{\Upsilon}(s))(t-s)^{\mu_*-1}|ds,$$
$$\leq [\frac{(1-\mu_*)}{\aleph(\mu_*)}\mathbf{L}_\rho+\frac{\eta^{\mu_*}}{\aleph(\mu_*)\Gamma(\mu_*)}\mathbf{L}_\rho]||\Upsilon-\tilde{\Upsilon}||,$$
$$=\Lambda||\Upsilon-\tilde{\Upsilon}||. \tag{14}$$

Thus, the proof is complete, from contraction principle, the operator has a unique fixed point. Consequently, 2-age group smoke transmission model has unique solution. □

5. Hyers-Ulam stability results for the 2-age group smoke transmission model

The stability of the proposed system will be examined in this section of the paper with regard to HU and generalised HU stability. Recently, HU type stability is one of the most intriguing. The HU stability was initially described by [27] and later generalized by Rassias [28]. In this analysis, we apply HU type stability for the 2-age group smoke transmission model.

Definition 5.1. The 2-age group smoke transmission model is HU stable if there $\exists\ \delta > 0$ and let $\Upsilon \in \boldsymbol{B}_*$ be any solution of inequality

$${}_0^{ABC}D_t^{\mu_*}\Upsilon(t)-\Psi(t,\Upsilon(t)) \leq \delta,\ \ \forall t \in [0,\eta]; \tag{15}$$

and $\exists$ unique solution $\tilde{\Upsilon}$ of system (4) with $\lambda_q > 0$, such that

$$||\Upsilon-\tilde{\Upsilon}|| \leq \lambda_q\delta,\ \ \forall t \in [0,\eta]. \tag{16}$$

Definition 5.2. Further, if $\exists\ \phi \in C(R,R)$, such that $\phi(0)=0$ for any solution Υ of (15) and $\tilde{\Upsilon}$ be unique solution of (4), such that

$$||\Upsilon-\tilde{\Upsilon}|| \leq \phi(\delta), \tag{17}$$

then the system (4) is generalized HU stable.

Remark 5.3. If $\exists\ \chi(t) \in C([0,\eta],R)$, then $\Upsilon \in \boldsymbol{B}_*$ satisfies inequality (15) suppose that,
(*i*) $|\chi(t)| \leq \delta$, for all $t \in [0,\eta]$,
(*ii*) ${}_0^{ABC}D_t^{\mu_*}\Upsilon(t) = \Psi(t,\Upsilon(t))+\chi(t)\ \forall\ t \in [0,\eta]$.

We now take a look at the system (4) perturbation equation, which is as follows:

$$\begin{cases} {}^{ABC}_{0}D_{t}^{\mu_*}\Upsilon(t) = \Psi(t,\Upsilon(t)) + \chi(t), \\ \Upsilon(0) = \Upsilon_0. \end{cases} \tag{18}$$

We require the following relation to continue our analysis.

Lemma 5.4. *From system (18),the following result holds.*

$$|\Upsilon(t) - \mathbf{A}_p\Psi(t,\Upsilon(t))| \leq \left[\frac{(1-\mu_*)}{\nabla(\mu_*)} + \frac{\eta^{\mu_*}}{\nabla(\mu_*)\Gamma(\mu_*)}\right]\delta.$$

Proof. Using Lemma 2.4, relatively, the solution of perturb Eq. (18) is given as;

$$\Upsilon(t) = \Upsilon_0 + {}^{ABC}_{0}I_t^{\mu_*}\Psi(t,\Upsilon(t)) + {}^{ABC}_{0}I_t^{\mu_*}\chi(t).$$

Now, from the knowledge of (9), we deduce the following

$$\begin{aligned} |\Upsilon(t) - \mathbf{A}_p\Psi(t,\Upsilon(t))| &\leq \left[\frac{(1-\mu_*)}{\aleph(\mu_*)}|\chi(t)| + \frac{\eta^{\mu_*}}{\aleph(\mu_*)\Gamma(\mu_*)}\int_0^t (t-s)^{1-\mu_*}|\chi(t)|ds\right] \\ &\leq \left[\frac{(1-\mu_*)}{\aleph(\mu_*)} + \frac{\eta^{\mu_*}}{\aleph(\mu_*)\Gamma(\mu_*)}\right]\delta. \ \square \end{aligned} \tag{19}$$

□

Theorem 5.5. *The system (4) is HU stable, if there exists*

$$\Lambda = \left[\frac{(1-\mu_*)}{\aleph(\mu_*)}\mathbf{L}_\rho + \frac{\eta^{\mu_*}}{\aleph(\mu_*)\Gamma(\mu_*)}\mathbf{L}_\rho\right] < 1.$$

Proof. Let $\Upsilon \in \boldsymbol{B}_*$ be any solution and $\tilde{\Upsilon} \in \boldsymbol{B}_*$ be unique solution of (4), then

$$\begin{aligned} |\Upsilon(t) - \tilde{\Upsilon}(t)| &= |\Upsilon(t) - \mathbf{A}_p\tilde{\Upsilon}(t)| \\ &\leq |\Upsilon(t) - \mathbf{A}_p\Upsilon(t)| + |\mathbf{A}_p\Upsilon(t) - \mathbf{A}_p\tilde{\Upsilon}(t)| \\ &\leq \left[\frac{(1-\mu_*)}{\aleph(\mu_*)} + \frac{\eta^{\mu_*}}{\aleph(\mu_*)\Gamma(\mu_*)}\right]\delta + \left[\frac{(1-\mu_*)}{\aleph(\mu_*)}\mathbf{L}_\rho + \frac{\eta^{\mu_*}}{\aleph(\mu_*)\Gamma(\mu_*)}\mathbf{L}_\rho\right]||\Upsilon - \tilde{\Upsilon}|| \\ &\leq \frac{\left[\frac{(1-\mu_*)}{\aleph(\mu_*)} + \frac{\eta^{\mu_*}}{\aleph(\mu_*)\Gamma(\mu_*)}\right]}{1 - \left[\frac{(1-\mu_*)}{\aleph(\mu_*)}\mathbf{L}_\rho + \frac{\eta^{\mu_*}}{\aleph(\mu_*)\Gamma(\mu_*)}\mathbf{L}_\rho\right]}\delta. \end{aligned} \tag{20}$$

Thus,

$$||\Upsilon(t) - \tilde{\Upsilon}(t)|| \leq \frac{[\frac{(1-\mu_*)}{\aleph(\mu_*)} + \frac{\eta^{\mu_*}}{\aleph(\mu_*)\Gamma(\mu_*)}]}{1 - [\frac{(1-\mu_*)}{\aleph(\mu_*)}\mathbf{L}_\rho + \frac{\eta^{\mu_*}}{\aleph(\mu_*)\Gamma(\mu_*)}\mathbf{L}_\rho]}\delta$$

Hence, we conclude that, system (4) is HU stable. Consequently, it is generalized HU stable. □

Definition 5.6. The system (4) is Hyers-Ulam-Rassias (HUR) stable for $\xi(\sigma) \in C([0,1],R)$, $\delta > 0$ and let $\Upsilon \in \boldsymbol{B}_*$ be any solution of inequality

$${}^{ABC}_{0}D_t^{\mu_*}\Upsilon(t) - \Psi(t,\Upsilon(t)) \leq \xi(t)\delta, \ \ \forall t \in [0,\eta]; \tag{21}$$

and also ∃ unique solution $\tilde{\Upsilon}$ of system (4) with $\lambda_q > 0$ then,

$$||\Upsilon - \tilde{\Upsilon}|| \leq \lambda_q\xi(t)\delta, \ \ \forall t \in [0,\eta]. \tag{22}$$

Definition 5.7. If ∃ $\nu \in C([0,\eta],R)$, with $\lambda_{q,\nu}$ and $\delta > 0$, for all Υ of system 21 and $\tilde{\Upsilon}$ be unique solution of (4), such that

$$||\Upsilon - \tilde{\Upsilon}|| \leq \lambda_{q,\nu}\nu(t), \forall\ t \in [0,\eta], \tag{23}$$

then Eq. (4) is generalized HUR stable.

Remark 5.8. If ∃ $\mu(t) \in C([0,\eta];R)$, and $\Upsilon \in \boldsymbol{B}_*$ satisfies inequality (21) such that,

(*i*) $|\mu(t)| \leq \delta\nu(t), \ \forall t \in [0,\eta]$.

(*ii*) ${}^{ABC}_{0}D_t^{\mu_*}\Upsilon(t) = \Psi(t,\Upsilon(t)) + \mu(t) \ \forall t \in [0,\eta]$.

We now take a look at the system (21) perturbation equation, which is as follows

$$\begin{cases} {}^{ABC}_{0}D_t^{\mu_*}\Upsilon(t) = \Psi(t,\Upsilon(t)) + \mu(t), \\ \Upsilon(0) = \Upsilon_0. \end{cases} \tag{24}$$

Lemma 5.9. *From system (24), the following result holds. Thus,*

$$|\Upsilon(t) - \mathbf{A}_p\Psi(t,\Upsilon(t))| \leq [\frac{(1-\mu_*)}{\aleph(\mu_*)} + \frac{\eta^{\mu_*}}{\aleph(\mu_*)\Gamma(\mu_*)}]\nu(t)\delta.$$

Proof. Using Lemma 2.4, relatively, the solution of perturb Eq. (24) is given as;

$$\Upsilon(t) = \Upsilon_0 + {}^{ABC}I_t^{\mu_*}\Psi(t,\Upsilon(t)) + {}^{ABC}I_t^{\mu_*}\nu(t).$$

Now, from the knowledge of (9), we deduce the following

$$\begin{aligned}|\Upsilon(t) - \mathbf{A}_p\Psi(t,\Upsilon(t))| &\leq \left[\frac{(1-\mu_*)}{\aleph(\mu_*)}|\nu(t)| + \frac{\eta^{\mu_*}}{\aleph(\mu_*)\Gamma(\mu_*)}\int_0^t (t-s)^{1-\mu_*}|\nu(t)|ds\right]\\ &\leq \left[\frac{(1-\mu_*)}{\aleph(\mu_*)} + \frac{\eta^{\mu_*}}{\aleph(\mu_*)\Gamma(\mu_*)}\right]\nu(t)\delta. \ \square\end{aligned} \tag{25}$$

□

Theorem 5.10. *The system (4) is HUR stable, if there exists* $\Lambda = \left[\frac{(1-\mu_*)}{\nabla(\mu_*)}\mathbf{L}_\rho + \frac{\eta^{\mu_*}}{\nabla(\mu_*)\Gamma(\mu_*)}\mathbf{L}_\rho\right] < 1.$

Proof. Let $\Upsilon \in \boldsymbol{B}_*$ be any solution and $\tilde{\Upsilon} \in \boldsymbol{B}_*$ be unique solution for system (4), such that

$$\begin{aligned}|\Upsilon(t) - \tilde{\Upsilon}(t)| &= |\Upsilon(t) - \mathbf{A}_p\tilde{\Upsilon}(t)|\\ &\leq |\Upsilon(t) - \mathbf{A}_p\Upsilon(t)| + |\mathbf{A}_p\Upsilon(t) - \mathbf{A}_p\tilde{\Upsilon}(t)|\\ &\leq [\frac{(1-\mu_*)}{\aleph(\mu_*)} + \frac{\eta^{\mu_*}}{\aleph(\mu_*)\Gamma(\mu_*)}]\nu(t)\delta + [\frac{(1-\mu_*)}{\aleph(\mu_*)}\mathbf{L}_\rho + \frac{\eta^{\mu_*}}{\aleph(\mu_*)\Gamma(\mu_*)}\mathbf{L}_\rho]||\Upsilon - \tilde{\Upsilon}||\\ &\leq \frac{[\frac{(1-\mu_*)}{\aleph(\mu_*)} + \frac{\eta^{\mu_*}}{\aleph(\mu_*)\Gamma(\mu_*)}]}{1 - [\frac{(1-\mu_*)}{\aleph(\mu_*)}\mathbf{L}_\rho + \frac{\eta^{\omega}}{\aleph(\mu_*)\Gamma(\mu_*)}\mathbf{L}_\rho]}\nu(t)\delta.\end{aligned} \tag{26}$$

Thus,

$$||\Upsilon(t) - \tilde{\Upsilon}(t)|| \leq \frac{[\frac{(1-\mu_*)}{\aleph(\mu_*)} + \frac{\eta^{\mu_*}}{\aleph(\mu_*)\Gamma(\mu_*)}]}{1 - [\frac{(1-\mu_*)}{\aleph(\mu_*)}\mathbf{L}_\rho + \frac{\eta^{\omega}}{\aleph(\mu_*)\Gamma(\mu_*)}\mathbf{L}_\rho]}\nu(t)\delta.$$

Hence, we conclude that, the system (4) is HUR stable. Consequently, it is generalized HUR stable. □

6. Numerical scheme for the 2-age group smoke transmission model

In this part, we will show the numerical solution for our considered 2-age group smoke transmission model, involving ABC-fractional operator, using the two-step Lagrange interpolation. See [33], for details about the numerical scheme. Taking the initial condition with respect to the operator ${}^{ABC}I_0^{\mu_*}$, we convert the 2-age group smoke transmission model (2) to fractional integral equations as

$$\begin{cases} P_1(t) - P_1(0) = {}^{ABC}I_t^{\mu_*}\Psi_1(t,P_1(t)),\\ L_E(t) - Q_1(0) = {}^{ABC}I_t^{\mu_*}\Psi_2(t,Q_1(t)),\\ I_U(t) - S_1(0) = {}^{ABC}I_t^{\mu_*}\Psi_3(t,S_1(t)),\\ I_D(t) - R_1(0) = {}^{ABC}I_t^{\mu_*}\Psi_4(t,R_1(t)),\\ I_T(t) - U_1(0) = {}^{ABC}I_t^{\mu_*}\Psi_5(t,U_1(t)),\\ P_2(t) - P_2(0) = {}^{ABC}I_t^{\mu_*}\Psi_6(t,P_2(t)),\\ Q_2(t) - Q_2(0) = {}^{ABC}I_t^{\mu_*}\Psi_7(t,Q_2(t)),\\ S_2(t) - S_2(0) = {}^{ABC}I_t^{\mu_*}\Psi_8(t,S_2(t)),\\ R_2(t) - R_2(0) = {}^{ABC}I_t^{\mu_*}\Psi_9(t,R_2(t)),\\ U_2(t) - U_2(0) = {}^{ABC}I_t^{\mu_*}\Psi_{10}(t,U_2(t)), \end{cases} \tag{27}$$

therefore we have the following

$$\begin{aligned}P_1(t) &= P_1(0) + \frac{1-\mu_*}{\aleph(\mu_*)}\Psi_1(t,P_1(t)) + \frac{\mu_*}{\aleph(\mu_*)\Gamma(\mu_*)}\int_0^t \Psi_1(s,P_1(s))(t-s)^{\mu_*-1}ds,\\ Q_1(t) &= Q_1(0) + \frac{1-\mu_*}{\aleph(\mu_*)}\Psi_2(t,Q_1(t)) + \frac{\mu_*}{\aleph(\mu_*)\Gamma(\mu_*)}\int_0^\sigma \Psi_2(s,Q_1(s))(t-s)^{\mu_*-1}ds,\\ S_1(t) &= S_1(0) + \frac{1-\mu_*}{\aleph(\mu_*)}\Psi_3(t,S_1(t)) + \frac{\mu_*}{\aleph(\mu_*)\Gamma(\mu_*)}\int_0^t \Psi_3(s,S_1(s))(t-s)^{\mu_*-1}ds,\end{aligned}$$

$$R_1(t) = R_1(0) + \frac{1-\mu_*}{\aleph(\mu_*)}\Psi_4(t, R_1(t)) + \frac{\mu_*}{\aleph(\mu_*)\Gamma(\mu_*)}\int_0^{\sigma}\Psi_4(s, R_1(s))(t-s)^{\mu_*-1}ds,$$
$$U_1(t) = U_1(0) + \frac{1-\mu_*}{\aleph(\mu_*)}\Psi_5(t, U_1(t)) + \frac{\mu_*}{\aleph(\mu_*)\Gamma(\mu_*)}\int_0^{t}\Psi_5(s, U_1(s))(t-s)^{\mu_*-1}ds,$$
$$P_2(t) = P_2(0) + \frac{1-\mu_*}{\aleph(\mu_*)}\Psi_6(t, P_2(t)) + \frac{\mu_*}{\aleph(\mu_*)\Gamma(\mu_*)}\int_0^{t}\Psi_6(s, P_2(s))(t-s)^{\mu_*-1}ds,$$
$$Q_2(t) = Q_2(0) + \frac{1-\mu_*}{\aleph(\mu_*)}\Psi_7(t, Q_2(t)) + \frac{\mu_*}{\aleph(\mu_*)\Gamma(\mu_*)}\int_0^{t}\Psi_7(s, Q_2(s))(t-s)^{\mu_*-1}ds,$$
$$S_2(t) = S_2(0) + \frac{1-\mu_*}{\aleph(\mu_*)}\Psi_8(t, S_2(t)) + \frac{\mu_*}{\aleph(\mu_*)\Gamma(\mu_*)}\int_0^{t}\Psi_8(s, S_2(s))(t-s)^{\mu_*-1}ds,$$
$$R_2(t) = R_2(0) + \frac{1-\mu_*}{\aleph(\mu_*)}\Psi_9(t, R_2(t)) + \frac{\mu_*}{\aleph(\mu_*)\Gamma(\mu_*)}\int_0^{t}\Psi_9(s, R_2(s))(t-s)^{\mu_*-1}ds,$$
$$U_2(t) = U_2(0) + \frac{1-\mu_*}{\aleph(\mu_*)}\Psi_{10}(t, U_2(t)) + \frac{\mu_*}{\aleph(\mu_*)\Gamma(\mu_*)}\int_0^{\sigma}\Psi_{10}(s, U_2(s))(t-s)^{\mu_*-1}ds, \tag{28}$$

The ABC integral of Lemma 2.4 can be reproduced using the basic principles of calculus, taking into account the ABC derivative under the Cauchy problem.

$$\Upsilon(t) = \Upsilon_0 + \frac{1-\mu_*}{\aleph(\mu_*)}\Psi(t, \Upsilon(t)) + \frac{\mu_*}{\aleph(\mu_*)\Gamma(\mu_*)}\int_0^{t}\Psi(s, \Upsilon(s))(t-s)^{\mu_*-1}ds. \tag{29}$$

Taking the point $t_{(z^*+1)} = (z^*+1)h$ and $t_{z^*} = z^*h,\ z^* = 0, 1, 2, \ldots$, with h being the time step, we deduce

$$\begin{aligned}
\Upsilon(t_{z^*+1}) &= \Upsilon_0 + \frac{1-\mu_*}{\aleph(\mu_*)}\Psi(t, \Upsilon(t)) + \frac{\mu_*}{\aleph(\mu_*)\Gamma(\mu_*)}\int_0^{t}\Psi(s, \Upsilon(s))(t-s)^{\mu_*-1}ds,\\
&= \Upsilon_0 + \frac{1-\mu_*}{\aleph(\mu_*)}\Psi(t_{z^*}, \Upsilon(t_{z^*})) + \frac{\mu_*}{\aleph(\mu_*)\Gamma(\mu_*)}\int_0^{t_{z^*+1}}\Psi(\theta, \Theta(\theta))(t_{z^*+1}-\theta)^{\mu_*-1}d\theta,\\
&= \Upsilon_0 + \frac{1-\mu_*}{\aleph(\mu_*)}\Psi(t_{z^*}, \Upsilon(t_{z^*})) + \frac{\mu_*}{\aleph(\mu_*)\Gamma(\mu_*)}\sum_{r_*=0}^{z^*}\int_{t_{r_*}}^{t_{z^*+1}}\Psi(\theta, \Theta(\theta))(t_{z^*+1}-\theta)^{\mu_*-1}d\theta.
\end{aligned}$$

At the point $[t_{z^*}, t_{(z^*+1)}]$, the two term Lagrange polynomial is given as follows;

$$\begin{aligned}
\Phi_{r_*}(\theta) &= \frac{\theta - t_{r_*+1}}{t_{r_*} - t_{r_*+1}}\Psi(t_{r_*}, \Upsilon(t_{r_*})) - \frac{\theta - t_{r_*}}{t_{r_*} - t_{r_*+1}}\Psi(t_{r_*-1}, \Upsilon(t_{r_*-1})),\\
&= \frac{\Psi(t_{r_*}, \Upsilon(t_{r_*}))}{h}(\theta - t_{r_*+1}) - \frac{\Psi(t_{r_*-1}, \Upsilon(t_{r_*-1}))}{h}(\theta - t_{r_*}),\\
&\simeq \frac{\Psi(t_{r_*}, \Upsilon_{r_*})}{h}(\theta - t_{r_*+1}) - \frac{\Psi(t_{r_*-1}, \Upsilon_{r_*-1})}{h}(\theta - t_{r_*}).
\end{aligned} \tag{30}$$

Taking the approximation solution of (30) into (30);

$$\begin{aligned}
\Upsilon(t_{z^*+1}) = \Upsilon_0 &+ \frac{1-\mu_*}{\aleph(\mu_*)}\Psi(t_{z^*}, \Upsilon(t_{z^*})) + \frac{\mu_*}{\aleph(\mu_*)\Gamma(\mu_*)}\\
&\times \sum_{r_*=0}^{z^*}\Bigg[\frac{\Psi(t_{r_*}, \Upsilon_{r_*})}{h}\int_{t_{r_*}}^{t_{r_*+1}}(\theta - t_{r_*-1})(t_{z^*+1}-\theta)^{\mu_*-1}d\theta\\
&- \frac{\Psi(t_{r_*-1}, \Upsilon_{r_*-1})}{h}\int_{t_{r_*}}^{t_{r_*+1}}(\theta - t_{r_*})(t_{z^*+1}-\theta)^{\mu_*-1}d\theta\Bigg].
\end{aligned} \tag{31}$$

For simplicity, we solve the integral equations in the (31) as follow;

$$\begin{aligned}
\Omega_{\mu_*, r_*, 1} &= \int_{t_{r_*}}^{t_{r_*+1}}(\theta - t_{r_*-1})(t_{z^*+1}-\theta)^{\mu_*-1}d\theta,\\
\Omega_{\mu_*, r_*, 2} &= \int_{t_{r_*}}^{t_{r_*+1}}(\theta - t_{r_*})(t_{z^*+1}-\theta)^{\mu_*-1}d\theta.
\end{aligned} \tag{32}$$

Using integration by substitution, we deduce from (32) as follow;

$$\begin{aligned}
\Omega_{\mu_*, r_*, 1} &= h^{\mu_*+1}\frac{(z^*+1-r_*)^{\mu_*}(z^*-r_*+2+\mu_*) - (z^*-r_*)^{\mu_*}(z^*-r_*+2+2\mu_*)}{\mu_*(\mu_*+1)},\\
\Omega_{\mu_*, r_*, 2} &= h^{\mu_*+1}\frac{(z^*+1-r_*)^{\mu_*+1} - (z^*-r_*)^{\mu_*}(z^*-r_*+1+\mu_*)}{\mu_*(\mu_*+1)}.
\end{aligned} \tag{33}$$

Here, knowing $\Omega_{\mu_*,r_*,1}$ and $\Omega_{\mu_*,r_*,2}$, we simply substitute into (31), this provides us the numerical scheme seen below;

$$\begin{aligned}\Upsilon(t_{z^*+1}) &= \Upsilon_0 + \frac{1-\mu_*}{\aleph(\mu_*)}\Psi(t_{z^*},\Upsilon(t_{z^*})) + \frac{\mu_*}{\aleph(\mu_*)}\\ &\times \sum_{r_*=0}^{z^*}\left[\frac{h^{\mu_*}\Psi(t_{r_*},\Upsilon_{r_*})}{\Gamma(\mu_*+2)}((z^*+1-r_*)^{\mu_*}(z^*-r_*+2+\mu_*)-(z^*-r_*)^{\mu_*}(z^*-r_*+2+2\mu_*))\right]\\ &-\frac{\mu_*}{\aleph(\mu_*)}\sum_{r_*=0}^{z^*}\left[\frac{h^{\mu_*}\Psi(t_{r_*-1},\Upsilon_{r_*-1})}{\Gamma(\mu_*+2)}((z^*+1-r_*)^{\mu_*+1}-(z^*-r_*)^{\mu_*}(z^*-r_*+1+\mu_*))\right].\end{aligned} \tag{34}$$

Therefore, the numerical scheme for our fractional order 2-age group smoke transmission model in terms of ABC-fractional derivative is as follows;

$$\begin{aligned}P_{1_{z^*+1}} &= P_1(0) + \frac{1-\mu_*}{\aleph(\mu_*)}\Psi_1(t_{z^*},P_1(t_{z^*})) + \frac{\mu_*}{\aleph(\mu_*)}\\ &\times \sum_{r_*=0}^{z^*}\left[\frac{h^{\mu_*}\Psi_1(t_{r_*},P_{1_{r_*}})}{\Gamma(\mu_*+2)}((z^*+1-r_*)^{\mu_*}(z^*-r_*+2+\mu_*)-(z^*-r_*)^{\mu_*}(z^*-r_*+2+2\mu_*))\right]\\ &-\frac{\mu_*}{\aleph(\mu_*)}\sum_{r_*=0}^{z^*}\left[\frac{h^{\mu_*}\Psi_1(t_{r_*-1},P_{1_{r_*-1}})}{\Gamma(\mu_*+2)}((z^*+1-r_*)^{\mu_*+1}-(z^*-r_*)^{\mu_*}(z^*-r_*+1+\mu_*))\right].\\ Q_{1_{z^*+1}} &= Q_1(0) + \frac{1-\mu_*}{\aleph(\mu_*)}\Psi_2(t_{z^*},Q_1(t_{z^*})) + \frac{\mu_*}{\aleph(\mu_*)}\\ &\times \sum_{r_*=0}^{z^*}\left[\frac{h^{\mu_*}\Psi_2(t_{r_*},Q_{1_{r_*}})}{\Gamma(\mu_*+2)}((z^*+1-r_*)^{\mu_*}(z^*-r_*+2+\mu_*)-(z^*-r_*)^{\mu_*}(z^*-r_*+2+2\mu_*))\right]\\ &-\frac{\mu_*}{\aleph(\mu_*)}\sum_{r_*=0}^{z^*}\left[\frac{h^{\mu_*}\Psi_2(t_{r_*-1},Q_{1_{r_*-1}})}{\Gamma(\mu_*+2)}((z^*+1-r_*)^{\mu_*+1}-(z^*-r_*)^{\mu_*}(z^*-r_*+1+\mu_*))\right].\\ S_{1_{z^*+1}} &= S_1(0) + \frac{1-\mu_*}{\aleph(\mu_*)}\Psi_3(t_{z^*},S_1(t_{z^*})) + \frac{\mu_*}{\aleph(\mu_*)}\\ &\times \sum_{r_*=0}^{z^*}\left[\frac{h^{\mu_*}\Psi_3(t_{r_*},S_{1_{r_*}})}{\Gamma(\mu_*+2)}((z^*+1-r_*)^{\mu_*}(z^*-r_*+2+\mu_*)-(z^*-r_*)^{\mu_*}(z^*-r_*+2+2\mu_*))\right]\\ &-\frac{\mu_*}{\aleph(\mu_*)}\sum_{r_*=0}^{z^*}\left[\frac{h^{\mu_*}\Psi_3(t_{r_*-1},S_{1_{r_*-1}})}{\Gamma(\mu_*+2)}((z^*+1-r_*)^{\mu_*+1}-(z^*-r_*)^{\mu_*}(z^*-r_*+1+\mu_*))\right].\end{aligned} \tag{35}$$

$$\begin{aligned}R_{1_{z^*+1}} &= R_1(0) + \frac{1-\mu_*}{\aleph(\mu_*)}\Psi_4(t_{z^*},R_1(t_{z^*})) + \frac{\mu_*}{\aleph(\mu_*)}\\ &\times \sum_{r_*=0}^{z^*}\left[\frac{h^{\mu_*}\Psi_4(t_{r_*},R_{1_{r_*}})}{\Gamma(\mu_*+2)}((z^*+1-r_*)^{\mu_*}(z^*-r_*+2+\mu_*)-(z^*-r_*)^{\mu_*}(z^*-r_*+2+2\mu_*))\right]\\ &-\frac{\mu_*}{\aleph(\mu_*)}\sum_{r_*=0}^{z^*}\left[\frac{h^{\mu_*}\Psi_4(t_{r_*-1},R_{1_{r_*-1}})}{\Gamma(\mu_*+2)}((z^*+1-r_*)^{\mu_*+1}-(z^*-r_*)^{\mu_*}(z^*-r_*+1+\mu_*))\right].\\ U_{1_{z^*+1}} &= U_1(0) + \frac{1-\mu_*}{\aleph(\mu_*)}\Psi_5(t_{z^*},U_1(t_{z^*})) + \frac{\mu_*}{\aleph(\mu_*)}\\ &\times \sum_{r_*=0}^{z^*}\left[\frac{h^{\mu_*}\Psi_5(t_{r_*},U_{1_{r_*}})}{\Gamma(\mu_*+2)}((z^*+1-r_*)^{\mu_*}(z^*-r_*+2+\mu_*)-(z^*-r_*)^{\mu_*}(z^*-r_*+2+2\mu_*))\right]\\ &-\frac{\mu_*}{\aleph(\mu_*)}\sum_{r_*=0}^{z^*}\left[\frac{h^{\mu_*}\Psi_5(t_{r_*-1},U_{1_{r_*-1}})}{\Gamma(\mu_*+2)}((z^*+1-r_*)^{\mu_*+1}-(z^*-r_*)^{\mu_*}(z^*-r_*+1+\mu_*))\right].\\ P_{2_{z^*+1}} &= P_2(0) + \frac{1-\mu_*}{\aleph(\mu_*)}\Psi_6(t_{z^*},P_1(t_{z^*})) + \frac{\mu_*}{\aleph(\mu_*)}\\ &\times \sum_{r_*=0}^{z^*}\left[\frac{h^{\mu_*}\Psi_6(t_{r_*},P_{2_{r_*}})}{\Gamma(\mu_*+2)}((z^*+1-r_*)^{\mu_*}(z^*-r_*+2+\mu_*)-(z^*-r_*)^{\mu_*}(z^*-r_*+2+2\mu_*))\right]\end{aligned}$$

$$- \frac{\mu_*}{\aleph(\mu_*)} \sum_{r_*=0}^{z^*} \left[\frac{h^{\mu_*} \Psi_6(t_{r_*-1}, P_{2_{r_*-1}})}{\Gamma(\mu_*+2)} ((z^*+1-r_*)^{\mu_*+1} - (z^*-r_*)^{\mu_*}(z^*-r_*+1+\mu_*)) \right].$$

$$Q_{2_{z^*+1}} = Q_2(0) + \frac{1-\mu_*}{\aleph(\mu_*)} \Psi_7(t_{z^*}, Q_2(t_{z^*})) + \frac{\mu_*}{\aleph(\mu_*)} \times \sum_{r_*=0}^{z^*} \left[\frac{h^{\mu_*} \Psi_7(t_{r_*}, Q_{2_{r_*}})}{\Gamma(\mu_*+2)} ((z^*+1-r_*)^{\mu_*}(z^*-r_*+2+\mu_*) - (z^*-r_*)^{\mu_*}(z^*-r_*+2+2\mu_*)) \right]$$

$$- \frac{\mu_*}{\aleph(\mu_*)} \sum_{r_*=0}^{z^*} \left[\frac{h^{\mu_*} \Psi_7(t_{r_*-1}, Q_{2_{r_*-1}})}{\Gamma(\mu_*+2)} ((z^*+1-r_*)^{\mu_*+1} - (z^*-r_*)^{\mu_*}(z^*-r_*+1+\mu_*)) \right].$$

$$S_{2_{z^*+1}} = S_2(0) + \frac{1-\mu_*}{\aleph(\mu_*)} \Psi_8(t_{z^*}, S_2(t_{z^*})) + \frac{\mu_*}{\aleph(\mu_*)} \times \sum_{r_*=0}^{z^*} \left[\frac{h^{\mu_*} \Psi_8(t_{r_*}, S_{1_{r_*}})}{\Gamma(\mu_*+2)} ((z^*+1-r_*)^{\mu_*}(z^*-r_*+2+\mu_*) - (z^*-r_*)^{\mu_*}(z^*-r_*+2+2\mu_*)) \right]$$

$$- \frac{\mu_*}{\aleph(\mu_*)} \sum_{r_*=0}^{z^*} \left[\frac{h^{\mu_*} \Psi_8(t_{r_*-1}, S_{2_{r_*-1}})}{\Gamma(\mu_*+2)} ((z^*+1-r_*)^{\mu_*+1} - (z^*-r_*)^{\mu_*}(z^*-r_*+1+\mu_*)) \right]. \tag{36}$$

$$R_{2_{z^*+1}} = R_2(0) + \frac{1-\mu_*}{\aleph(\mu_*)} \Psi_9(t_{z^*}, R_2(t_{z^*})) + \frac{\mu_*}{\aleph(\mu_*)} \times \sum_{r_*=0}^{z^*} \left[\frac{h^{\mu_*} \Psi_9(t_{r_*}, R_{2_{r_*}})}{\Gamma(\mu_*+2)} ((z^*+1-r_*)^{\mu_*}(z^*-r_*+2+\mu_*) - (z^*-r_*)^{\mu_*}(z^*-r_*+2+2\mu_*)) \right]$$

$$- \frac{\mu_*}{\aleph(\mu_*)} \sum_{r_*=0}^{z^*} \left[\frac{h^{\mu_*} \Psi_9(t_{r_*-1}, R_{2_{r_*-1}})}{\Gamma(\mu_*+2)} ((z^*+1-r_*)^{\mu_*+1} - (z^*-r_*)^{\mu_*}(z^*-r_*+1+\mu_*)) \right].$$

$$U_{2_{z^*+1}} = U_2(0) + \frac{1-\mu_*}{\aleph(\mu_*)} \Psi_{10}(t_{z^*}, U_2(t_{z^*})) + \frac{\mu_*}{\aleph(\mu_*)} \times \sum_{r_*=0}^{z^*} \left[\frac{h^{\mu_*} \Psi_{10}(t_{r_*}, U_{2_{r_*}})}{\Gamma(\mu_*+2)} ((z^*+1-r_*)^{\mu_*}(z^*-r_*+2+\mu_*) - (z^*-r_*)^{\mu_*}(z^*-r_*+2+2\mu_*)) \right]$$

$$- \frac{\mu_*}{\aleph(\mu_*)} \sum_{r_*=0}^{z^*} \left[\frac{h^{\mu_*} \Psi_{10}(t_{r_*-1}, U_{2_{r_*-1}})}{\Gamma(\mu_*+2)} ((z^*+1-r_*)^{\mu_*+1} - (z^*-r_*)^{\mu_*}(z^*-r_*+1+\mu_*)) \right]. \tag{37}$$

7. Numerical results and discussion for the 2-age group smoke transmission model

This section of the study presents the numerical results and some discussions regarding the approximate solution of the 2-age group smoke transmission model. We compute the model associated with the ABC-fractional operator $\mu_* \in (0.1)$ using the fractional Adams-Bashforth technique for numerical simulation. Here, we take some suitable initial conditions together with the parameter values as follows; $P_1(0) = 80$; $Q_1(0) = 27$; $S_1(0) = 21$; $R_1(0) = 30$; $U_1(0) = 32$; $P_2(0) = 60$; $Q_2(0) = 24$; $S_2(0) = 18$; $R_2(0) = 35$; $U_2(0) = 40$. The numerical results given in Fig. 4–9 show numerical simulations of the solution of our model as a function of time for different ABC-fractional order. It is worth noting that, the prediction depends on the value of the ABC-fractional order also beside the theoretical parameters. From our observation, the memory effect of the system increases when the ABC-fractional order μ_* is lowered from 1, and so the infection to smoke-related disease grows slowly. The ABC-fractional operator μ_* impacts the dynamics that define patients affected with smoke-related disease due to the memory property of fractional derivatives. When ABC-fractional order μ_* tends to 0, we noticed that the infection's maximum levels are reduced.

From Fig. 4(a),4(c) and Fig. 5(a),5(c) we noticed that the rate at which 1-Group become potential smoker and addicted to smoking was high as compared to 2-Group. The trajectories in Fig. 4(b) and Fig. 5(b) is proportional to the fractional operator. From Fig. 4(d) and Fig. 5(d), we observed high rate of 2-Group people quitting from smoking as compared to 1-Group. Fig. 4(e) and Fig. 5(e) shows major memory difference between 1-Group and 2-Group. In addition, when we choose different parameter values for β_1 and β_2 with fixed fractional operator $\mu_* = 0.90$. In Fig. 6–9, we observed different transmission between 1-Group and 2-Group. In Fig. 6, as we varied β_1, obviously, the rate at which 1-Group becomes smoker increases. On the other hand, when we varied β_1 resulted in a minimal transmission rate on the 2-Group smokers. In Fig. 6(e) and Fig. 7e, when β_1 is varied, we observed no significant impact. In Fig. 8 and Fig. 9, as we varied β_2, obviously, the rate at which 2-Group become smokers increases. On the other hand, when one varies β_2, the trajectory of smokers in the 1-Group reduces. This could be as result of the 2-Group have less contact with the public.

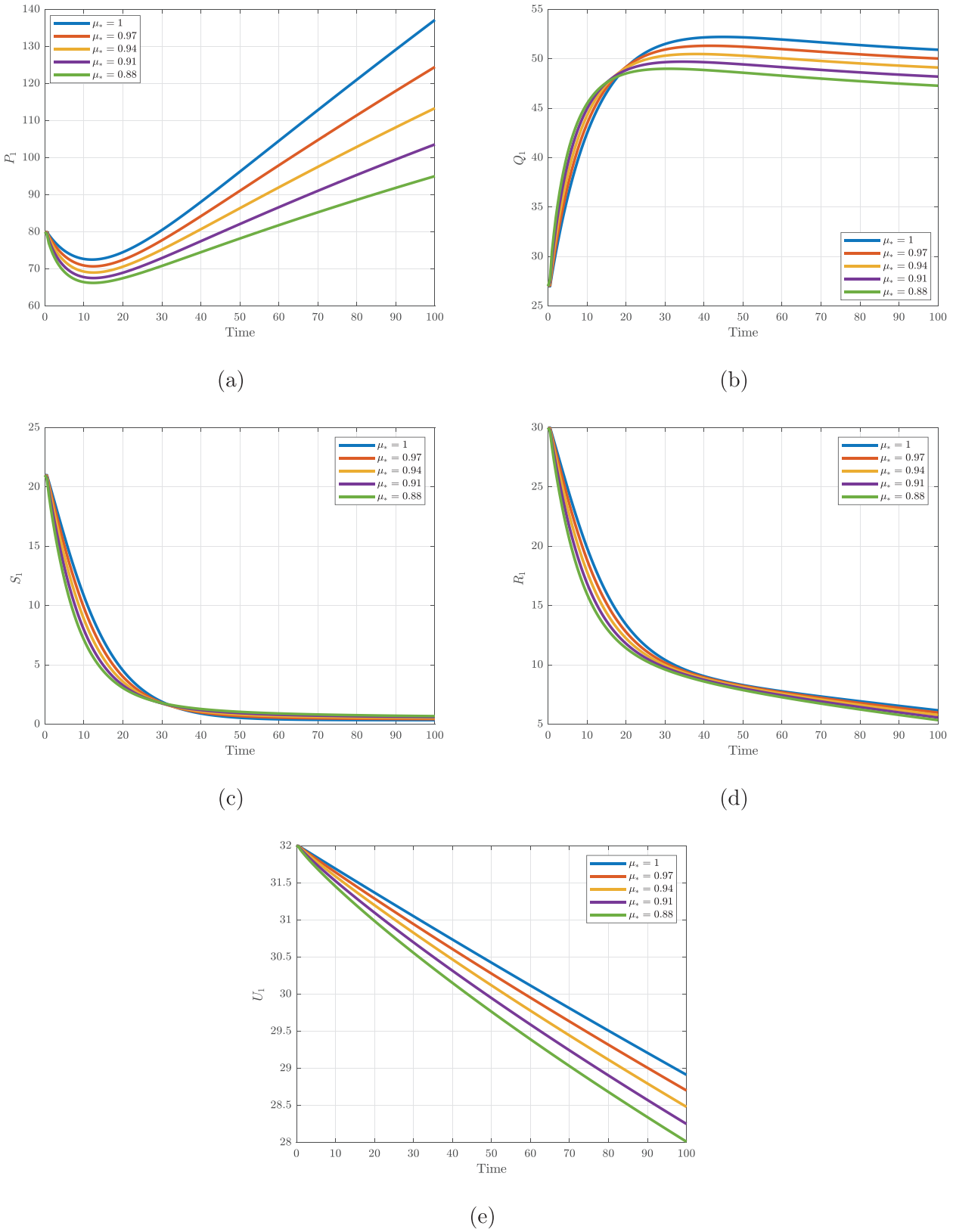

Fig. 4. Fractional dynamics of 1-Group classes at different fractional order μ_*.

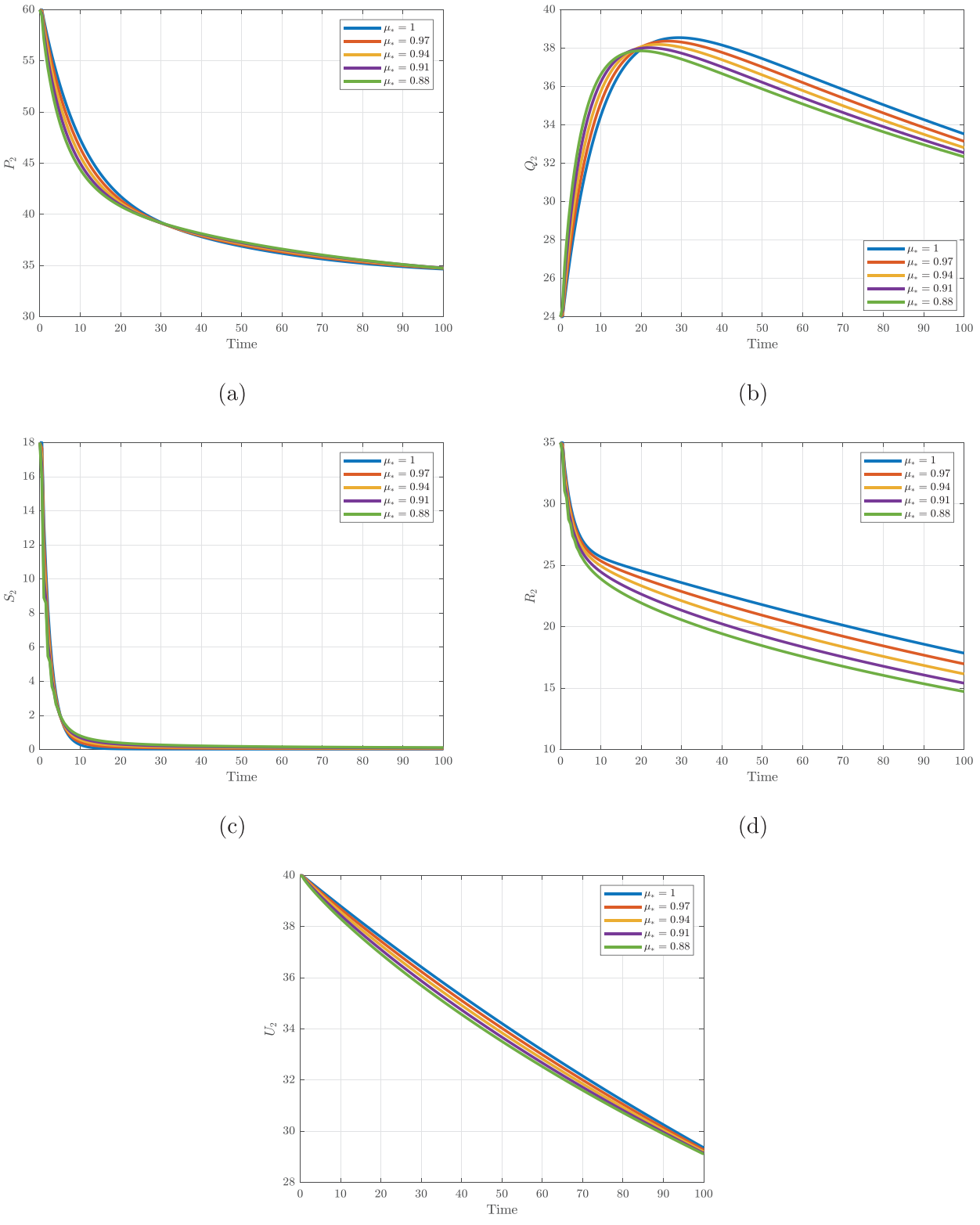

Fig. 5. Fractional dynamics of 2-Group classes at different fractional order μ_*.

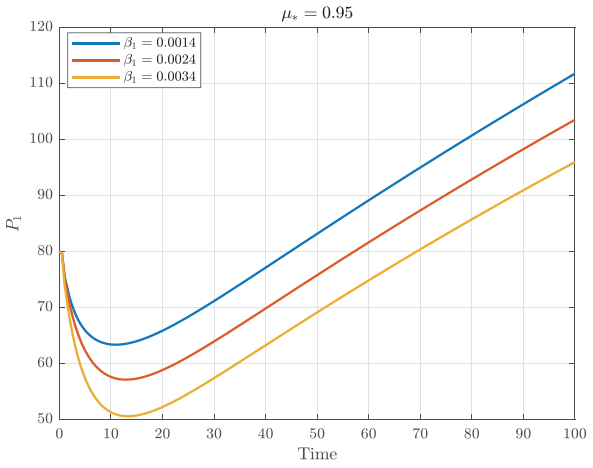

(a)

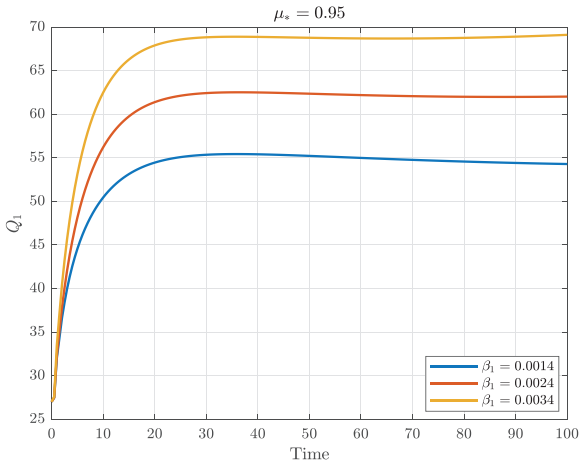

(b)

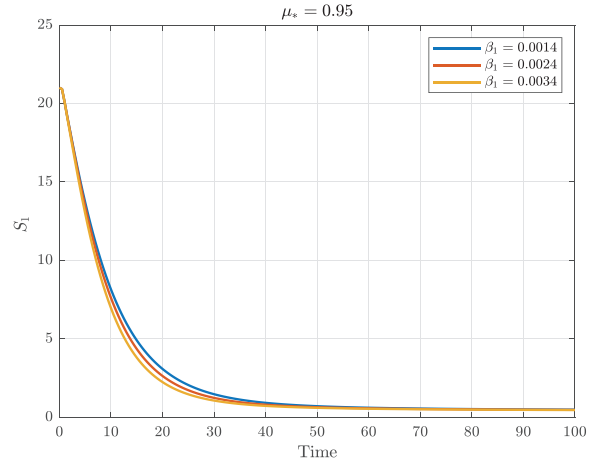

(c)

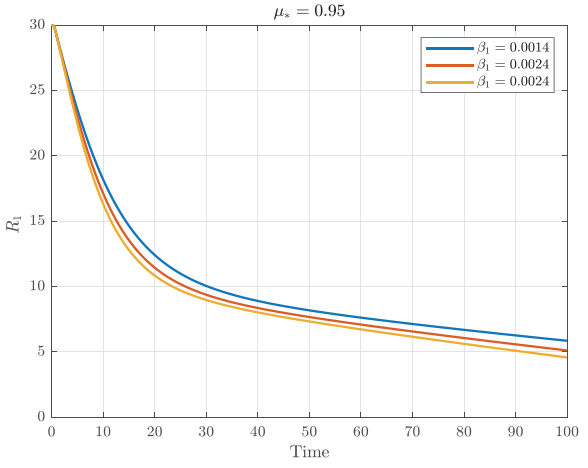

(d)

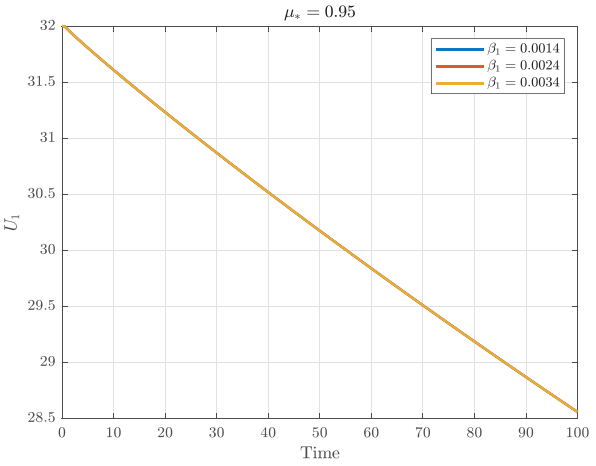

(e)

Fig. 6. Dynamics of 1-Group classes at different initial conditions for β_1 when operator is fixed at $\mu_* = 0.95$.

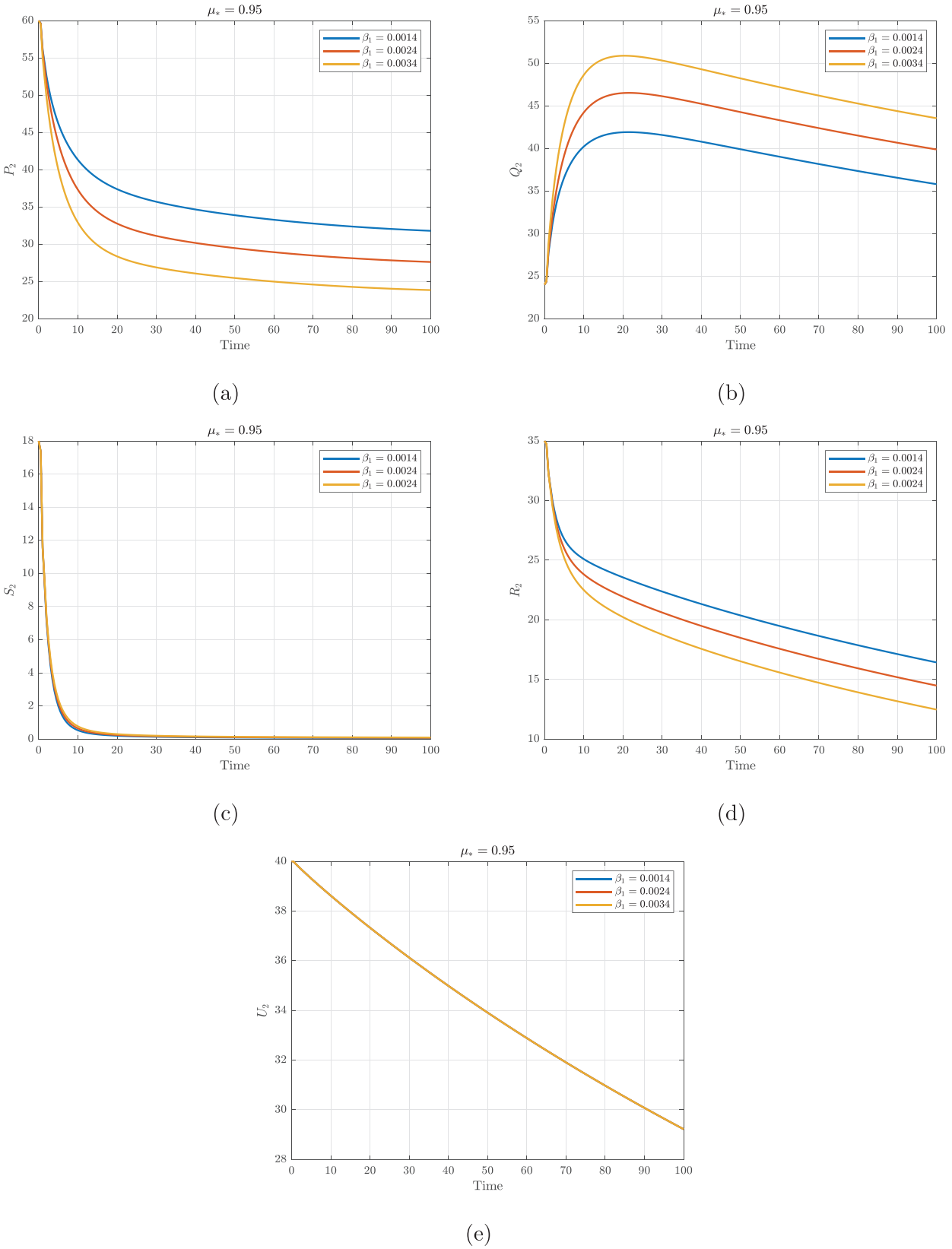

Fig. 7. Dynamics of 2-Group classes at different initial conditions for β_1 when operator is fixed at $\mu_* = 0.95$.

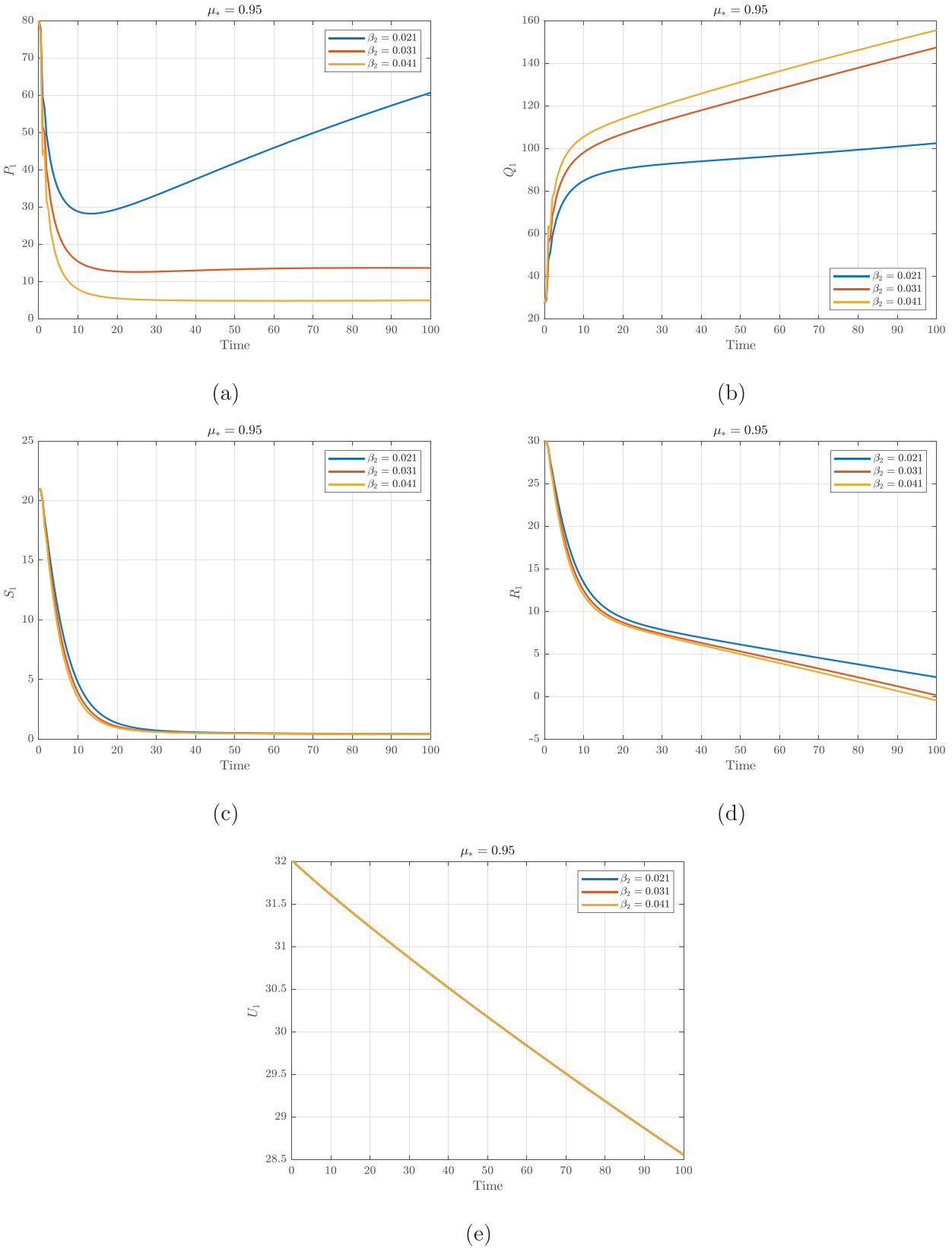

Fig. 8. Dynamics of 1-Group classes at different initial conditions for β_2 when operator is fixed at $\mu_* = 0.95$.

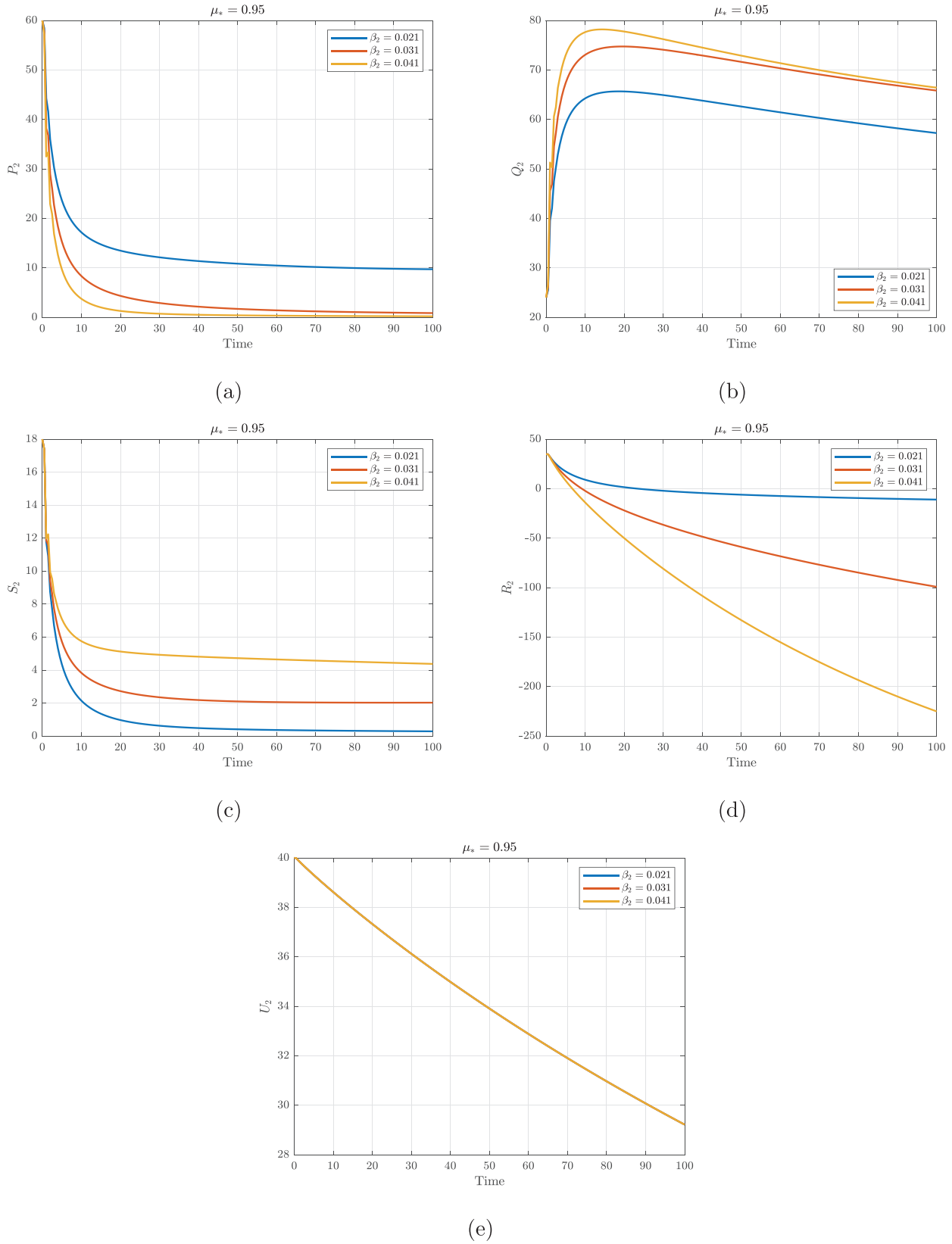

Fig. 9. Dynamics of 2-Group classes at different initial conditions for β_2 when operator is fixed at $\mu_* = 0.95$.

8. Conclusion

We have formulated dynamics of the 2-age group smoke transmission model under ABC-fractional order. By means of the fixed point theorem of Banach and Krasnoselskii's type, we proved the existence and uniqueness set of the solutions of the 2-age group smoke transmission model and the stability solutions by HU stability type. Numerical simulations with the assumption of specific parameters, we were able to achieve complex dynamics of the system by changing the ABC-fractional operators. Figures obtained demonstrate the simulations for the analytical solutions of the special 2-age group smoke model and notably depends on the ABC-fractional derivative. We come to the conclusion that the model can be modified to add the effects of campaigns like publicly funded programmes to avoid the smoking epidemic. It is feasible to pinpoint the age groups that should be addressed for a campaign to be most successful. Similarly, the model could also be useful in setting up age-dependent treatment programmes. In the future, this work could be used to study different fractional operators and fractal-fractional optimal control with real data.

Declaration of Competing Interest

The writers state that they do not have any competing interests.

CRediT authorship contribution statement

Emmanuel Addai: Conceptualization, Methodology, Formal analysis, Writing – original draft, Writing – review & editing. **Lingling Zhang:** Supervision, Methodology, Formal analysis, Writing – review & editing. **Joshua K. K. Asamoah:** Supervision, Methodology, Formal analysis, Writing – original draft, Writing – review & editing. **John Fiifi Essel:** Writing – review & editing.

Data availability

No data was used for the research described in the article.

Acknowledgements

This paper is supported by Key R&D program of Shanxi Province (International Cooperation, 201903D421042) and Research Project Supported by Shanxi Scholarship Council of China (2021-030). The first author appreciate Mr. Samuel Peprah, Mr. Dominic Kwame Agyemang as well as Janet Agyemang for their support.

References

[1] K.S. Miller, B. Ross, An Introduction to the Fractional Calculus and Fractional Differential Equations, Wiley, 1993.
[2] A.A. Kilbas, H. Srivastava, J. Trujillo, Theory and Application of Fractional Differential Equations, Vol. 204, Elsevier, 2006.
[3] J.K.K. Asamoah, E. Okyere, E. Yankson, A.A. Opoku, A. Adom-Konadu, E. Acheampong, Y.D. Arthur, Non-fractional and fractional mathematical analysis and simulations for q fever, Chaos, Solitons & Fractals 156 (2022) 111821.
[4] Y. Chen, F. Liu, Q. Yu, T. Li, Review of fractional epidemic models, Appl Math Model 97 (2021) 281–307, doi:10.1016/j.apm.2021.03.044.
[5] M. Caputo, M. Fabrizio, A new definition of fractional derivative without singular kernel, Progr. Fract. Differ. App. 1 (2) (2015) 1–13, doi:10.12785/pfda/010201.
[6] S. Alizadeh, D. Baleanu, S. Rezapour, Analyzing transient response of the parallel RCL circuit by using the caputo-fabrizio fractional derivative, Adv. Differ. Equ. 55 (2020), doi:10.1186/s13662-020-2527-0.
[7] D. Baleanu, A. Jajarmi, H. Mohammad, S. Rezapour, A new study on the mathematical modelling of human liver with caputo-fabrizio fractional derivative, Chaos Solit. Fract. 134 (109705) (2020) 1–7, doi:10.1016/j.chaos.2020.109705.
[8] A. Atangana, D. Baleanu, New fractional derivatives with nonlocal and non-singular kernel: theory and application to heat transfer model, Therm. Sci. 220 (2) (2016) 763–769, doi:10.2298/TSCI160111018A.
[9] A. Atangana, J.F. Gómez-Aguilar, A new derivative with normal distribution kernel: theory, methods and applications, Physica A: Stat. Mech. Appl. 476 (2017) 1–14, doi:10.1016/j.physa.2017.02.016.
[10] T.M.S. Thabet, S.A. Mohammed, et al., Study of transmission dynamics of COVID-19 mathematical model under ABC fractional order derivative, Results Phys. 19 (2020) 103507, doi:10.1186/j.rinp.2020.103507.
[11] A. Atangana, Non validity of index law in fractional calculus: a fractional differential operator with Markovian and non-Markovian properties, Physica A 505 (2018) 688–706, doi:10.1016/j.physa.2018.03.056.
[12] A. Atangana, J.F. Gomez-Aguilar, Fractional derivatives with no-index law property: application to chaos and statistics, Chaos, Solit. Fract. 114 (2018) 516–535, doi:10.1016/j.chaos.2018.07.033.
[13] K.M. Saad, J.F. Gomez-Aguilar, Analysis of reaction-diffusion system via a new fractional derivative with non-singular kernel, Physica A Stat. Mech. Appl. 509 (2018) 703–716, doi:10.1016/j.physa.2018.05.137.
[14] F. Jarad, T. Abdeljawad, Z. Hammouch, On a class of ordinary differential equations in the frame of Atangana-Baleanu fractional derivative, Chaos, Solit. Fract. 117 (2018) 16–20, doi:10.1016/j.chaos.2018.10.006.
[15] M. Sher, K. Shah, Z.A. Khan, H. Khan, A. Khan, Computational and theoretical modeling of the transmission dynamics of novel COVID-19 under mittag-leffler power law, Alexandria Engineering Journal 59 (2020) 3133–3147, doi:10.1016/j.aej.2020.07.014.
[16] J.K.K. Asamoah, Fractal-fractional model and numerical scheme based on newton polynomial for Q fever disease under Atangana-Baleanu derivative, Results Phys. 34 (2022) 105189.
[17] V.F. Morales-Delgadoa, et al., Mathematical modeling of the smoking dynamics using fractional differential equations with local and nonlocal kernel, J Nonl Sci Appl 11 (8) (2018) 1004–1014, doi:10.22436/jnsa.011.08.06.
[18] M. Abdullah, A. Ahmad, N. Raza, et al., Approximate solution and analysis of smoking epidemic model with Caputo fractional derivatives, Int. J. Appl. Comput. Math. 4 (112) (2018) 1–16, doi:10.1007/s40819-018-0543-5.

[19] G.A.K. van Voorn, B.W. Kooi, Smoking epidemic eradication in an eco-epidemiological dynamical model, Ecol. Complexity 14 (2013) 180–189, doi:10.1016/j.ecocom.2013.01.008.
[20] A. Lahrouz, L. Omari, D. Kiouach, A. Belmaati, Deterministic and stochasticstability of a mathematical model of smoking, Stat. Prob. Letters 81 (2011) 1276–1284, doi:10.1016/J.SPL.2011.03.029.
[21] P.H. Chen, H.R. White, R.J. Pandina, Predictors of smoking cessation from adolescence into young adulthood, Addic. Behaviors 26 (2001) 517–529, doi:10.1016/S0306-4603(00)00142-8.
[22] Z. Gu, Qualitative behavior of giving up smoking models, Bulletin of the Malaysian Math. Sci. Society 34 (2) (2011) 403–415. http://eudml.org/doc/244432
[23] R. Ullah, et al., Dynamical features of a mathematical model on smoking, J. Appl. Environ. Biol. Sci. 6 (1) (2016) 92–96.
[24] O. Sharomi, A.B. Gumel, Curtailing smoking dynamics: a mathematical modeling approach, Appl. Math. Comput. 195 (2) (2008) 475–499, doi:10.1016/j.amc.2007.05.012.
[25] S.A. Khan, K. Shah, G. Zaman, F. Jarad, Existence theory and numerical solutions to smoking model under Caputo-Fabrizio fractional derivative, Chaos 29 (1) (2019) 1–10, doi:10.1063/1.5079644. 013128
[26] H. Ritchie, M. Roser, "smoking". published online at ourworldindata.org, 2013, Retrieved from: 'https://ourworldindata.org/smoking' [Online Resource].
[27] D.H. Hyers, On the stability of the linear functional equation, Proc. Natl. Acad. Sci. USA 27 (4) (1941) 222–224.
[28] T.M. Rassias, On the stability of the linear mapping in banach spaces, Proc. Amer. Math. Soc. 72 (2) (1978) 297–300.
[29] M. Paavola, E. Vartiainen, P. Puska, Smoke cessation between teenage years and adulthood, Health Edu. Research 16 (1) (2001) 49–57.
[30] D. Baleanu, M.H. Abadi, A. Jajarmi, K.Z. Vahid, J.J. Nieto, A new comparative study on the general fractional model of COVID-19 with isolation and quarantine effects, Alexandria Engineering Journal 61 (6) (2022) 4779–4791.
[31] L. Zhang, E. Addai, J. Ackora-Prah, Y.D. Arthur, J.K.K. Asamoah, Fractional-order ebola-malaria coinfection model with a focus on detection and treatment rate, Comput Math Methods Med (2022) 2022.
[32] F. Ozkose, M. Yavuz, et al., Fractional order modelling of omicron SARS-CoV-2 variant containing heart attack effect using real data from the united kingdom, Chaos, Solitons & Fractals. 167 (2023) 111954.
[33] A. Atangana, S.I. Araz, New numerical scheme with newton polynomial: Theory, Methods and Applications, Academic Press, 2021.
[34] G.T. Tilahuna, W.A. Woldegerimab, N. Mohammed, A fractional order model for the transmission dynamics of hepatitis B virus with two-age structure in the presence of vaccination, Arab J. of Basic and App. Sci. 28 (1) (2021) 87–106, doi:10.1080/25765299.2021.1896423.